



Available online at www.sciencedirect.com

ScienceDirect

Geochimica et Cosmochimica Acta 332 (2022) 138-155

Geochimica et Cosmochimica Acta

www.elsevier.com/locate/gca

LIP volcanism (not anoxia) tracked by Cr isotopes during Ocean Anoxic Event 2 in the proto-North Atlantic region

Lucien Nana Yobo ^{a,b,*}, Chris Holmden ^c, Alan D. Brandon ^b, Kimberly V. Lau ^d, James S. Eldrett ^e, Steven Bergman ^{f,1}

a Department of Geology and Geophysics, Texas A&M University, College Station, TX, USA
 b Department of Earth and Atmospheric Sciences, University of Houston, Houston, TX, USA
 c Saskatchewan Isotope Laboratory, Department of Earth Science, University of Saskatchewan, Saskatoon, Canada
 d Department of Geosciences and Earth and Environmental Systems Institute, The Pennsylvania State University, University Park, PA, USA
 c Shell Global Solutions International B.V., Netherlands
 f SCB GeoSciences, Vashon, WA, USA

Received 10 February 2022; accepted in revised form 9 June 2022; Available online 20 June 2022

Abstract

Chromium is a redox sensitive element that exhibits a large range of isotopic compositions in Earth's surface environments because of Cr(VI)-Cr(III) transformations. This property of Cr has been exploited as a tracer of Earth's oxygenation history using marine sediments. However, paleoredox applications using Cr are difficult to implement due to its complicated cycling, which creates spatial variability in seawater δ⁵³Cr values. Applications are further hindered by the potential for variability in the major inputs of Cr, such as submarine volcanism, to mask redox processes. Two previous reports of negative excursions in sedimentary δ⁵³Cr values during the middle Cretaceous Ocean Anoxic Event 2 (OAE 2) demonstrate these complications. Observed negative shifts in marine sediments conflict with the positive shifts expected in response to the increased drawdown of isotopically light Cr(III) prompted by the expansion of anoxic depositional sinks. In this study, a marine carbonate succession cored from the Eagle Ford Formation in Texas, USA, in the southern part of the Western Interior Seaway, depicts the negative 1.5‰ δ⁵³Cr excursion occurring in two steps, with the second step reaching peak minimum values indistinguishable from isotopically unfractionated igneous sources. In contrast to published δ⁵³Cr records, each step stratigraphically matches proxy evidence for increased eruption frequency and/or intensity of volcanic activity using combined ¹⁸⁷Os/¹⁸⁸Os, ⁸⁷Sr/⁸⁶Sr and Os concentration proxies previously measured from the same core, supporting higher inputs of volcanically sourced Cr to the oceans as the driver for the negative Cr isotope excursion.

Crown Copyright © 2022 Published by Elsevier Ltd. All rights reserved.

Keywords: Cr isotopes; OAE 2; Anoxia; Hydrothermal; Paleoclimate; Paleoceanography; Cretaceous

1. INTRODUCTION

Chromium (Cr) is a redox sensitive element with isotopic variation in Earth surface environments that reflects

changes in its oxidation state (Ellis et al., 2002). This property of Cr has been exploited as a tracer of Earth's

oxygenation history using marine sediments (Crowe et al., 2013; Frei et al., 2009; Gilleaudeau et al., 2016; Planavsky et al., 2014) and paleosols (Berger and Frei, 2014; Babechuk et al., 2017; Toma et al., 2019). Its development as a paleoredox proxy, however, continues to be a challenge

due to its complicated modern cycling (Bonnand et al., 2013; Scheiderich et al. 2015), redox dependent

^{*} Corresponding author.

E-mail address: lnanayobo@tamu.edu (L. Nana Yobo).

¹ Formerly, Shell Technology Center, Houston, TX, USA.

(Ellis et al., 2002; Sikora et al., 2008; Døssing et al., 2011; Zink et al., 2010; Basu et al., 2014; Wang et al., 2016; Huang et al., 2021) and independent (Saad et al., 2017; Babechuk et al., 2018) sources of isotopic fractionation, multiple pathways for Cr enrichment and isotopic fractionation in marine sediments (Holmden et al., 2016; Farkaš et al., 2018; Remmelzwaal et al. 2019), and difficult assessments of the preservation potential of exogenic Cr signals in geological archives (Albut et al., 2018, 2019).

The dominant oxidation state of chromium in the oceans is Cr(VI) in the form of the thermodynamically stable chromate and hydrogenchromate oxyanions (CrO₄², HCrO₄) (Elderfield, 1970; Cranston and Murray, 1978). Reduction to reactive Cr(III) species (e.g., Cr (OH)₂⁺) (Elderfield, 1970) occurs in biologically productive surface waters and oxygen depleted zones (Campbell and Yeats, 1981; Cranston, 1983; Jeandel and Minster, 1984; Murray et al., 1983; Mugo and Orians, 1993; Rue et al., 1997; Sirinawin et al., 2000; Semeniuk et al., 2016). Light isotopes are favored in the produced Cr(III) leaving the residual pool of Cr(VI) enriched in heavy isotopes. The greater attraction of Cr(III) for surfaces of particles causes separation of Cr isotopes between surface and deep waters through the action of the biological pump. This leads to increased total dissolved Cr concentrations ([Cr]_T = Cr(VI) + Cr(III) and decreased ⁵³Cr/⁵²Cr ratios (reported in delta notation as δ^{53} Cr values) with depth in the oceans (Scheiderich et al., 2015; Moos and Boyle, 2019).

Seawater δ^{53} Cr values range between ~ 0.6 and 1.6% (Bonnand et al., 2013; Scheiderich et al., 2015; Goring-Harford et al., 2018; Moos and Boyle, 2019; Rickli et al., 2019; Nasemann et al., 2020; Janssen et al., 2020,2021) and are inversely correlated with [Cr]_T on a global scale in $\ln[\text{Cr}]_{\text{T}} - \delta^{53}\text{Cr}$ space with a slope of $-0.80 \pm 0.03\%$ (Scheiderich et al., 2015). The strong correlation of the global array and long oceanic Cr residence time (9,000–39,00 0 years; Campbell and Yeats, 1981) justifies treatment of the ocean Cr cycle as a closed system with the fractionation factor governing Cr(VI) reduction in the oceans estimated from the slope of the array (Scheiderich et al., 2015). This interpretation implies a single unique process of Cr(VI) reduction in the oceans, or range of processes with similar fractionation factors, and low export fractions of Cr(III) compared to total dissolved Cr. The low apparent fractionation of $-1.3 \pm 0.1\%$ estimated using δ^{53} Cr measurements of co-existing Cr(VI) and Cr(III) species in oxygen depleted waters of the Eastern Tropical North Pacific (Huang et al., 2021) is consistent with this interpretation.

Generally, Cr(VI) reduction drives seawater Cr compositions up the global Cr array (toward low [Cr]_T and high δ^{53} Cr), if accompanied by scavenging and export of the produced Cr(III). Regeneration of Cr(III) drives deep waters down the global Cr array (toward high [Cr]_T and low δ^{53} Cr). The separation of Cr isotopes between surface and deep waters is damped by the strong tendency for Cr (III) to form soluble organic complexes (Nakayama et al.,1981; Sander and Koschinsky, 2000; Sander et al., 2003), reducing its export efficiency and improving the likelihood of re-oxidation to Cr(VI). This may occur on time scales of months to years using dissolved oxygen or hydro-

gen peroxide (Schroeder and Lee, 1975; Pettine and Millero, 1990). Only a fraction of the Cr(III) produced by Cr(VI) reduction is typically exported or removed to the sediment before re-oxidation to Cr(VI). This enables deep waters to remain on the global Cr array in a closed system.

The highest seawater δ^{53} Cr values reach $\sim 1.6\%$ in productive shelf regions, such as the Chukchi Sea (Scheiderich et al., 2015; Moos and Boyle, 2019), Oregon coast (Scheiderich et al. 2015), English Channel (Bonnand et al., 2013) and surface waters of the subarctic North Pacific (Janssen et al., 2020). Biological activity is implicated in the reduction of Cr(VI) in these regions, using organic matter, Fe(II), H₂O₂ and/or reactive oxygen species produced by the biota or by reactions with light (Semeniuk et al., 2016). The biogenic particles generated by photosynthesis are crucial for scavenging and export of Cr(III). Most of the burial of Cr(III) occurs in continental shelf seas and margins that are well oxygenated. Higher concentrations of Cr may be found in organic-rich marine sediments deposited beneath oxygen-depleted bottom waters where Cr(III) burial is more efficient (Murray et al., 1983; Rue et al., 1997; Moos and Boyle, 2019; Nasemann et al., 2020; Huang et al., 2021). Export or burial of Cr(III) elevates the δ^{53} Cr of seawater, locally, above the value in surrounding regions. It is also responsible on a global scale for raising the δ^{53} Cr of the ocean Cr reservoir above the level of its inputs, which is mostly continental weathering sources in the present day, such as rivers with a weighted average δ^{53} Cr value of 0.47 \pm 0.39‰ (1 s) (Toma et al., 2019). This compares to the mean of $\sim 0.9\%$ for the oceans. Thus, it is expected that during periods of globally increased productivity and expanded marine anoxia, seawater δ^{53} Cr values will increase and [Cr]_T will decrease in both shallow and deep ocean settings, and that these changes will be preserved in records of authigenic sedimentary Cr in different marine settings (e.g., Gueguen et al., 2016). This study further tests the predicted relationship using a well-known event in Earth's history.

Spanning the Cenomanian/Turonian boundary, the Cretaceous Oceanic Anoxic Event 2 (OAE 2 ~ 94.5 Ma) is recognized for widespread organic-rich black shale deposition (Schlanger and Jenkyns, 1976), and a global scale positive C isotope excursion indicative of increased organic carbon burial and elevated primary productivity in multiple locations (Fig. 1). Two previously published marine sedimentary records of OAE 2 failed to produce evidence for the positive shift in seawater δ^{53} Cr values predicted for more reducing oceans: (1) the Portland #1 core of the Western Interior Seaway (WIS) of North America collected from sediments representing a relatively shallow (<500 m water depth) and oxygenated epicontinental sea (Holmden et al., 2016), and (2) the site 1258 Ocean Drilling Project core collected from relatively deep (~1000 m) continental slope sediments at Demerara Rise, representing deposition beneath anoxic bottom waters along the southern margin of the proto-North Atlantic Ocean (Wang et al., 2016). Instead of sedimentary δ^{53} Cr values increasing in response to globally expanded marine anoxia, both records decreased during OAE 2. The proposed explanations conflict regarding the roles of redox conditions on Cr isotope

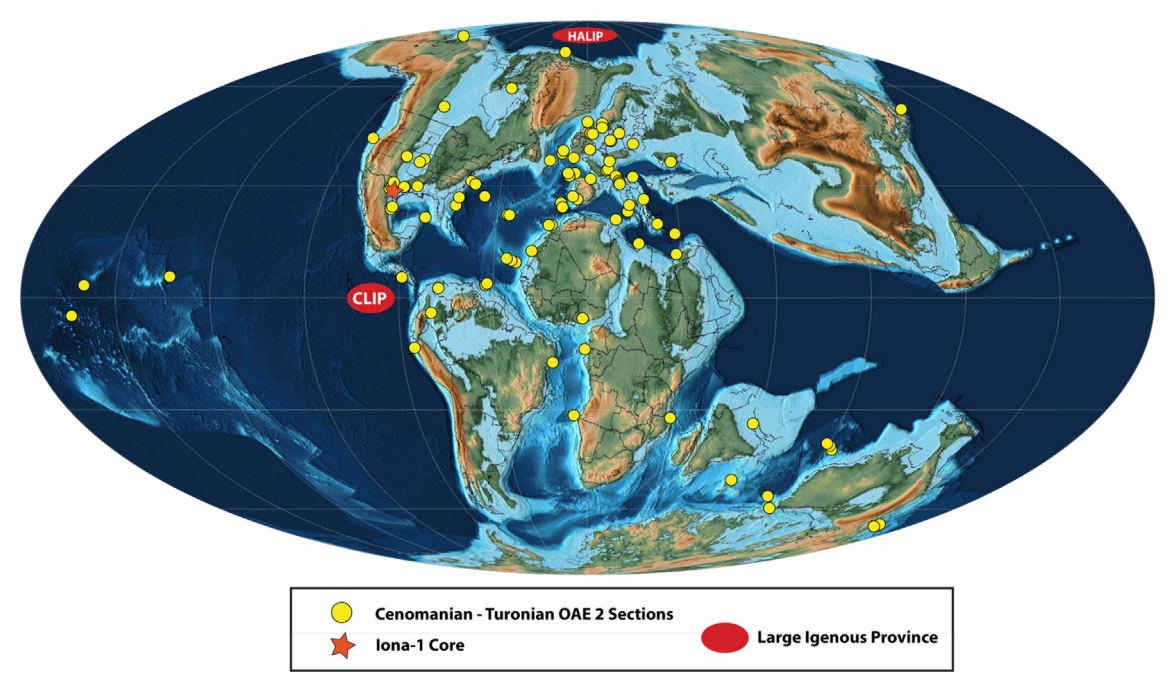


Fig. 1. Paleogeographic reconstruction from Scotese (2016) of late Cenomanian (~94 Ma) with identified sedimentary sections of Cenomanian–Turonian OAE 2 deposits (red dots) modified from Paez-Reyes et al. (2021). Also illustrated are the locations of the Iona-1 core and the following LIPs: CLIP, Caribbean Large Igneous Province; HALIP, High Arctic Large Igneous Province. (For interpretation of the references to colour in this figure legend, the reader is referred to the web version of this article.)

fractionation (Wang et al., 2016), volcanically derived sources of Cr to the oceans (Holmden et al., 2016), and oceanographic changes related to climate cooling (Jenkyns et al., 2017).

Building on previous studies linking OAE 2 to a massive episode of submarine volcanic activity, Holmden et al. (2016) proposed that eruptions of a Large Igneous Province (LIP) in the Caribbean—the proposed trigger for OAE 2 (Turgeon and Creaser, 2008)—caused increased hydrothermal inputs of Cr(III) to the oceans with a lower δ^{53} Cr value than the globally averaged Cr input from rivers. In fact, the peak-minimum δ^{53} Cr values reported in the Portland #1 core conspicuously overlapped those of the igneous inventory ($-0.12 \pm 0.10\%$, 2σ) (Schoenberg et al., 2008), consistent with increased fluxes of hydrothermal Cr(III) and other metals of basaltic affinity such as iron (Fe), manganese (Mn), copper (Cu), nickel (Ni) and cobalt (Co), which are anomalous in concentration in the same stratigraphic interval as the minimum in δ^{53} Cr values (Orth et al., 1993; Sinton and Duncan, 1997; Snow et al., 2005).

Wang et al. (2016) proposed an alternative hypothesis using their black shale record at Demerara Rise. In this record, the onset of the negative shift in 53 Cr values occurs stratigraphically above the negative shift in 187 Os/ 188 Os ratios used to signal the first increase in submarine volcanic activity associated with the emplacement of the Caribbean LIP. On this basis they discarded the volcanic Cr input hypothesis. They proposed instead that the negative δ^{53} Cr excursion resulted from a shift in the fraction of Cr removed by marine euxinic sinks compared to anoxic/suboxic sinks, supposing that euxinic sinks removed Cr(VI)

from the middle Cretaceous oceans with little or no isotopic fractionation.

Jenkyns et al. (2017) also questioned whether the LIP eruptions were responsible for the negative excursion in inferred seawater δ^{53} Cr values during OAE 2 with the observation that conspicuous enrichments of Cr and other redox sensitive metals occur together in a stratigraphic interval in the English Chalk succession in the Anglo-Paris Basin called the Plenus Cold Event (PCE). Their rationale for questioning a hydrothermal source was informed by debate over the global vs. local scale of the cooling, which they believed was global and therefore driven by decreased LIP activity (e.g., Jenkyns et al., 2017; Clarkson et al., 2018). With the oceans becoming better oxygenated in a cooler climate, Jenkyns et al. (2017) reasoned that redox sensitive trace metals could be expected to be released from formerly anoxic marine sediment. Using carbon isotope stratigraphy, they correlated the Cr-enriched interval in the English Chalks to the negative δ⁵³Cr excursion in the Portland #1 core in the WIS, which is also enriched in Cr. In contrast, O'Connor et al. (2020) argued that the PCE was more likely a local or regional phenomenon, supported by volcanic proxy evidence from records of changing sedimentary Os concentrations, initial ¹⁸⁷Os/¹⁸⁸Os ratios (Sullivan et al., 2020), ⁸⁷Sr/⁸⁶Sr ratios (Nana Yobo et al., 2021), and initial ¹⁴³Nd/¹⁴⁴Nd ratios (Zheng et al., 2013) indicating that volcanism increased during parts of the PCE. This interpretation of higher volcanism during the PCE interval is in line with earlier studies linking trace metal enrichments to buoyant metal-rich superplumes drawn into the proto-North Atlantic from greater LIP activity in the eastern Pacific (Sinton and Duncan, 1997; Snow et al., 2005). Therefore, the leading hypotheses of trace metal enrichment during the PCE directly conflict with regards to the roles of volcanism and by extension, climate.

To reexamine the impact of changing volcanism on the ocean Cr cycle during OAE 2, a new high-resolution δ^{53} Cr profile was reconstructed using samples from the Iona-1 core (Eldrett et al., 2015a,b) located near the southern gateway between the WIS and the proto-North Atlantic Ocean, approximately 1200 km to the south of the earlier studied Portland #1 core. Positive attributes of the Iona-1 core, including its location, shallow burial depth, stratigraphic completeness, and well-characterized sedimentology and geochemistry (Eldrett et al. 2014, 2015a,b; Minisini et al., 2018), provide a new opportunity to improve on the interpretation of the cause of the negative Cr isotope excursion. Sediment in the Iona-1 core preserve a continuous record of pelagic limestone, marlstone, and calcareous shale deposition between the onset of LIP volcanism and the onset of OAE 2, i.e., between the first negative shift in initial ¹⁸⁷Os/¹⁸⁸Os ratios in the core and the first positive shift in the sedimentary δ^{13} C values. These markers overlap in the Portland # 1 core due to a sedimentary hiatus (Jones et al., 2020). The Iona-1 core is more complete than Portland core in the WIS (Eldrett et al., 2015a,b) and offers the prospect of additional temporal details in reconstructed proxy records. Uncertain corrections for lithogenic Cr also create ambiguity in the shape of the published δ^{53} Cr profiles that hinders a detailed comparison of the fine structure of the negative δ^{53} Cr excursion with volcanic proxy indicators in both the Portland #1 and Demerara Rise cores. Moreover, as Cr and its isotopes are not expected to be homogenous in the Cretaceous oceans, it is unclear whether and to what extent the records of the Portland and Demerara Rise cores are globally significant which indicates the need for multiple δ^{53} Cr records to be compared. The new δ^{53} Cr data are better integrated with other proxies for the intensity of submarine volcanism from the same core (187Os/186Os, 87Sr/86Sr, and Os concentration; Sullivan et al., 2020; Nana Yobo et al., 2021). Together, these proxies provide a clearer picture of the timing and direction of volcanic intensity changes during OAE 2 and can determine relationships with trace element enrichments and perturbations in ocean Cr cycling.

2. GEOLOGICAL SETTING

The Iona-1 core was drilled on a carbonate shelf at the southern gateway to the WIS in present-day southwest Texas (Fig. 2; 29°13.51′N, 100°44.49′W). The core recovered 180 m of Lower Cenomanian to Lower Coniacian marine sedimentary rocks composed of marls and shales, with intermittent bentonite of the Boquillas Formation of the Eagle Ford Group (Eldrett et al., 2014). Sedimentation was ~1–4 cm kyr ⁻¹ and assumed to be relatively continuous during OAE 2 in the study setting (Eldrett et al., 2015a; Minisini et al., 2018). An age model for the Iona-1 core was constructed from rhythmically deposited interbedded limestones and marlstones interpreted to reflect orbi-

tally forced sedimentation patterns, supported by U-Pb zircon dating of bentonite beds (Eldrett et al. 2014, 2015a,b; Minisini et al., 2018). The marls are predominantly finely laminated and organic carbon is enriched in the marls of the lower Eagle Ford, becoming more bioturbated up core and during OAE 2 (Eldrett et al., 2014). The more organically lean limestones are interpreted to reflect more consistently oxygenated bottom waters during OAE 2 in this setting, which is supported by changes in the stratigraphic frequency of bioturbation, and the lower sedimentary Mo concentrations during OAE 2 in the study core. Higher Mo concentrations before OAE 2 are interpreted to reflect bottom water euxinic conditions (Eldrett et al., 2014, 2015a; Minisini et al., 2018). The depth of deposition across OAE 2 is interpreted to be consistently below storm wave base in a sediment-starved setting (100-200 m) (Minisini et al, 2018). The carbonate fraction of the sediment is mostly calcareous nannofossil ooze with planktic foraminifera and calcispheres indicative of hemipelagic deposition. Carbonate δ^{13} C values for the Iona-1 core range between +1% to +6% with δ^{18} O values averaging -5% (Eldrett et al., 2015b). The bulk carbonate δ^{13} C and δ¹⁸O values in the Iona-1 core are similar to well preserved tests of calcitic foraminifera reported in other locations in the WIS (Eldrett et al., 2015b and references therein). Hence, the O and C isotopic values in the carbonate fraction of the Iona-1 core likely reflect primary seawater values that have not been significantly altered by post-depositional diagenetic processes, specifically of the type that would lead to very low δ^{18} O values indicative of higher temperatures encountered during recrystallization during deep burial, or alteration in the presence of meteoric waters (Eldrett et al., 2015b). Further details on the sedimentology, stratigraphy, and hydrographic conditions can be found in Eldrett et al. (2014, 2015a, 2017) and Minisini et al. (2018).

3. METHODS

Core samples were hand powdered using an aluminum oxide mortar and pestle. Powders weighing between 0.5 and 1.0 g were treated with ammonium acetate solution to remove exchangeable Cr and other elements on particle surfaces and then rinsed with ultrapure water. The carbonate fractions were dissolved in ultrapure 1.0 N acetic acid following procedures described in Nana Yobo et al. (2021). The procedure was designed to minimize release of Cr from non-carbonate minerals such as clays, thereby minimizing the impact of detrital Cr corrections on the δ^{53} Cr values for seawater derived Cr in the sediments. The carbonate fractions were targeted because studies have shown that carbonate sediments in modern marine environments are enriched in seawater-derived Cr (Bonnand et al., 2013; Holmden et al., 2016; Farkaš et al., 2018; Klaebe et al., 2021; Wang et al., 2021), offset by a fractionation $(-0.46 \pm 0.14\%, 2\sigma)$ (Holmden et al., 2016).

The supernatant was treated with nitric acid to devolatilize the excess acetate, followed by analysis of Cr and Al concentrations by ICP-MS. The amount of Al released by the acetic acid technique was very small, and the carbonate δ^{53} Cr profile does not require a detrital correction. Sample

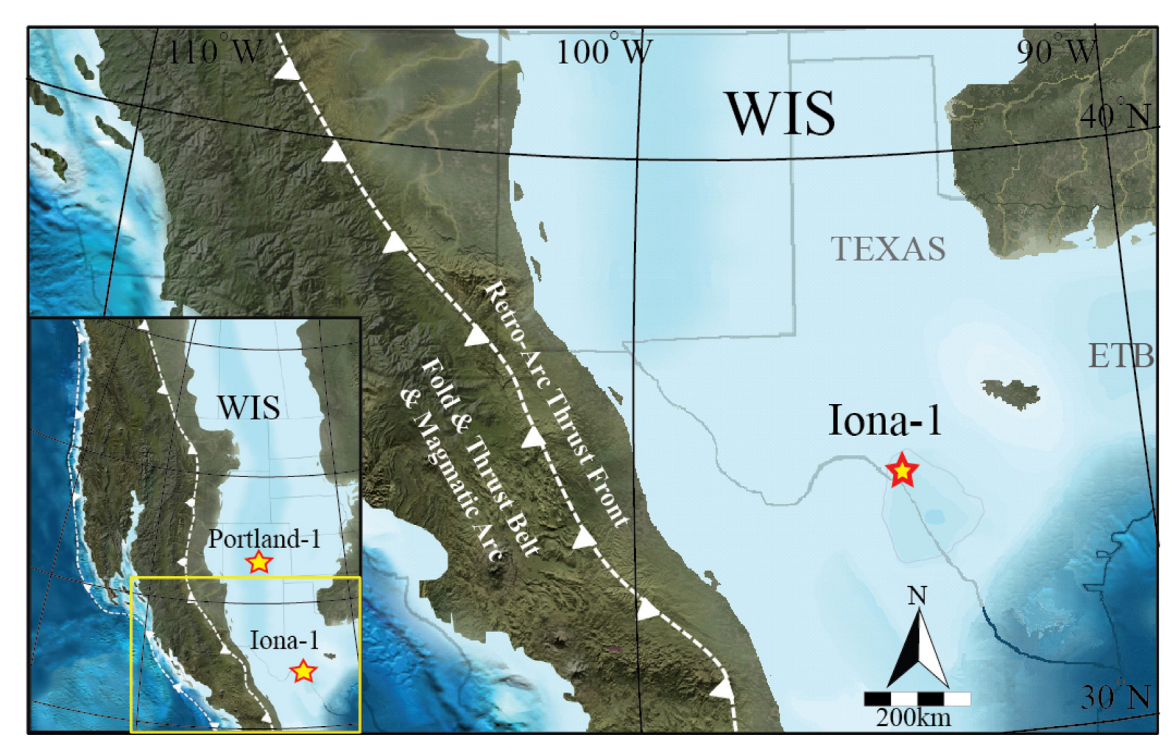


Fig. 2. Early Turonian paleogeographic map showing location of the Iona-1 and Portland #1 cores, modified from Eldrett et al. (2014). WIS, Western Interior Seaway.

aliquots were spiked with a $^{50}\text{Cr-}^{54}\text{Cr}$ tracer solution, and the Cr was separated from matrix Ca and other elements using procedures described in Holmden et al. (2016). The $^{53}\text{Cr/}^{52}\text{Cr}$ ratios were measured by thermal ionization mass spectrometry using a Thermo Scientific Triton instrument in the Saskatchewan Isotope Laboratory, University of Saskatchewan, using a double-spike technique detailed in Holmden et al. (2016), and reported as $\delta^{53}\text{Cr} = [(^{53}\text{Cr}/^{52}\text{Cr})_{sample}/(^{53}\text{Cr}/^{52}\text{Cr})_{standard} - 1] \times 1000$. The $\delta^{53}\text{Cr}$ value measured for a stock solution of NIST SRM 3112a was $-0.08 \pm 0.05\%$ (2 σ , n = 15).

4. RESULTS

4.1. δ^{53} Cr profile for the Iona-1 core compared to volcanic proxy indicators

The stratigraphic trends displayed by carbonate δ^{53} Cr record can be divided into four segments: A, B, C, and D (Fig. 3B). LIP volcanism begins at the base of segment A (~112 to 110 m), identified by synchronous stratigraphic shifts in sedimentary ¹⁸⁷Os/¹⁸⁸Os and ⁸⁷Sr/⁸⁶Sr ratios. The stratigraphic variability in the carbonate δ^{53} Cr values is small (~±0.2‰) in Segment A, and in the same range (~+1.6 to + 1.8‰) as lower down in the core. The steady baseline implies stable Cr cycling in the study setting for up to 500 kyr before OAE 2.

The first sign of a clear shift in carbonate δ^{53} Cr values coincides with the onset of the positive C isotope excursion at the base of Segment B that marks the onset of OAE 2. Here, δ^{53} Cr values decrease rapidly from $\sim +1.8\%$ to

 $\sim +0.7\%$ over a period of about 70 kyr. This brief stratigraphic interval of declining carbonate $\delta^{53} Cr$ values corresponds to the first of three intervals of elevated Os concentration with mantle-like $^{187} Os/^{188} Os$ initial ratios interpreted by Sullivan et al. (2020) to represent three peaks in frequency and/or intensity of submarine LIP volcanism (Fig. 3C; Sullivan et al., 2020), after which $\delta^{53} Cr$ values are stable for the remainder of Segment B, except for a single higher value of +1.35% at 106 m (Fig. 3B). The sample giving +1.35% correlates with the nominal middle peak in volcanism in the Os concentration profile, but there is uncertainty about the volcanic interpretation of the middle peak as the corresponding change in $^{187} Os/^{188} Os$ ratio is more ambiguous in this stratigraphic interval (Sullivan et al., 2020).

The youngest interval of Os enrichment, like that of the first volcanic interval at the base of OAE 2, shows a second clear shift to increasingly mantle-like $^{187}\mathrm{Os}/^{188}\mathrm{Os}$ ratios coinciding with a second negative shift in carbonate $\delta^{53}\mathrm{Cr}$ values captured in Segment C, this time reaching the peak minimum $\delta^{53}\mathrm{Cr}$ values (–0.04‰) of the excursion (Fig. 3B).

Segment D (103 to 80 m) records the simultaneous return to baseline $\delta^{53}Cr$ values and $^{187}Os/^{188}Os$ ratios (Fig. 3B). Within this segment, LIP volcanism is interpreted to have dramatically declined or stopped altogether, consistent with the very low Os concentrations in this segment beginning at about the midpoint of the $\delta^{13}C$ excursion. The post-excursion baseline is slightly lower in $^{187}Os/^{188}Os$ ratios than the pre-excursion baseline, indicating potentially higher background levels of volcanism than before

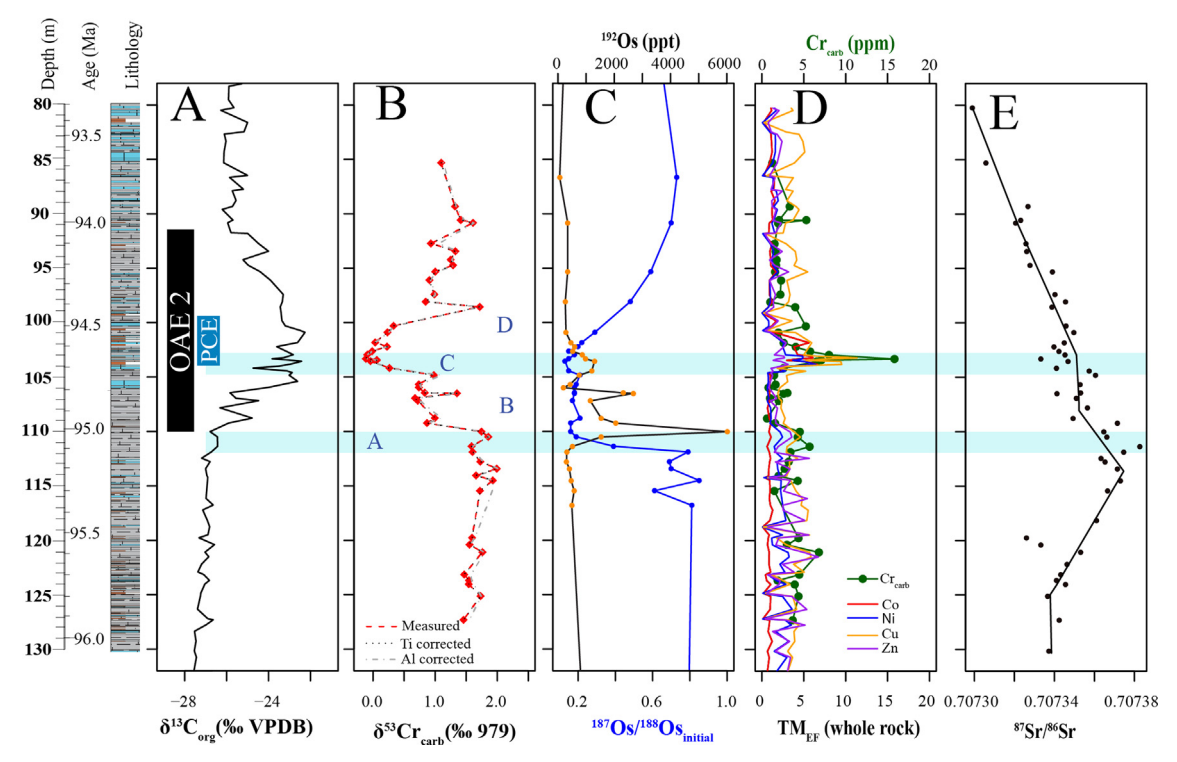


Fig. 3. Carbonate sedimentary profile through OAE 2 of the Iona-1 core. The stratigraphic column and age model are plotted against, δ^{13} Corg (Eldrett et al., 2014), carbonate δ^{53} Cr (this study), 187 Os/ 188 Os, 192 Os concentrations (Sullivan et al., 2020), Cr_{carb} (this study), trace metal EF normalized to Zr and average shale (Eldrett et al., 2014), and 87 Sr/ 86 Sr (Nana Yobo et al., 2021). The measured δ^{53} Cr (dashed red line) was corrected for lithogenic Cr using Ti (dotted black line) and for Al (dashed grey lines). The black bar represents the duration of the OAE 2 interval aand the blue bar represents the duration of the Plenus Cold Event (PCE) as correlated to the Iona-1 core by Jenkyns et al (2017). The δ^{53} Cr record is divided into 4 segments. Segment A represents the delay in onset of negative shift in δ^{53} Cr in relation to LIP eruption (70 kyr), as indicated by the decrease in 187 Os/ 188 Os and increased Os concentrations. Segment B is the first negative shift in Cr isotopes which corresponds to the middle of the negative shift in Os isotopes. Segment C represents the second shift to lower δ^{53} Cr and corresponds to both the PCE and an inferred increase in volcanism as indicated by a decrease in 187 Os/ 188 Os and increased Os concentrations. Finally, Segment D represents the end of volcanism signaled by a rise in 187 Os/ 188 Os, which occurs synchronously with a return to higher δ^{53} Cr values. (For interpretation of the references to colour in this figure legend, the reader is referred to the web version of this article.)

the event. The δ^{53} Cr value of $\sim 1.0\%$ in carbonates deposited after OAE 2 is also lower than before the event. The termination of the Os and Cr isotope excursions coincides with a change in the slope of the decreasing trend in 87 Sr/ 86 Sr ratio in the study core, which is also interpreted to reflect the decline or cessation of LIP volcanism (Nana Yobo et al., 2021).

5. DISCUSSION

5.1. δ^{53} Cr, Os concentration, 187 Os/ 188 Os and 87 Sr/ 86 Sr trends in the Iona-1 core

In the high-resolution record of the Iona-1 core, two clear steps in the negative excursion in carbonate δ^{53} Cr values are observed to coincide with two intervals of elevated Os concentrations with mantle-like ¹⁸⁷Os/¹⁸⁸Os ratios (Sullivan et al., 2020) at the bases of segments B and C (Fig. 3). This finding strengthens the volcanic driver hypothesis for the negative Cr isotope excursion during OAE 2 in this and two other published studies (Holmden et al., 2016; Wang et al., 2016). The earlier finding by

Wang et al. (2016) used to refute this hypothesis, which is that the onset of the negative δ^{53} Cr excursion occurs after the onset of the negative shift in ¹⁸⁷Os/¹⁸⁸Os ratios, is also a feature in the Iona-1 core (Segment A). The highresolution record demonstrates, however, that it is not the start of LIP volcanism that coincides with the decrease in carbonate δ^{53} Cr values but rather the first peak in volcanic intensity. This implies different thresholds of response for the ocean Os and Cr cycles to the volcanic perturbation, which depend on the respective sizes of the volcanically induced perturbations, and the mechanisms by which mantle Os and Cr are transmitted to seawater by submarine volcanic eruptions. For example, it has been suggested that high-temperature weathering of basalt alone cannot supply the large amounts of Os required to shift the ocean Os isotope balance towards the mantle input during OAE 2 (Turgeon and Creaser 2008), implying an alternative mantle source (Sharma et al., 2007) such as volatile magmatic Os (Krähenbühl et al., 1992). It is therefore the details of LIP sources and plumbing that may be responsible for controlling the supply of mantle-derived Os to the oceans during OAE 2.

Peculiarities in the supply of Cr to the oceans during LIP eruptions should probably not be discounted either. Recent work has shown that Cr(II), in the form of the neutral CrCl (OH) complex, is the dominant oxidation state of Cr in high temperature crustal fluids and is more soluble than Cr(III) (Huang et al., 2021). Though the modern residence time of Sr is, itself, poorly constrained (Peucker-Ehrenbrink and Fiske, 2019), it is at least two orders of magnitude greater than that of Os or Cr. Despite this large difference, covarying shifts in ⁸⁷Sr/⁸⁶Sr and ¹⁸⁷Os/¹⁸⁸Os ratios in the Iona-1 core indicate some combination of a lower oceanic Sr residence time and high Sr-flux perturbation associated with the LIP eruptions in the middle Cretaceous (Nana Yobo et al., 2021). Though the shifts in ⁸⁷Sr/⁸⁶Sr are subtle in comparison to Cr and Os isotopes, they are not imperceptible. Furthermore, the strong correlation between Cr isotopes and volcanic proxy indicators (187Os/188Os, Os concentration, trace metal anomalies and ⁸⁷Sr/⁸⁶Sr) continues up-core. The youngest volcanism pulse in Segment C is proposed in this study to drive carbonate δ^{53} Cr values to the igneous inventory value. Moreover, the cessation of volcanism at the base of the overlying segment D, which is signaled by the return to baseline ¹⁸⁷Os/¹⁸⁸Os ratios and low Os concentrations, is simultaneously indicated in a subtle shift of slope in the ⁸⁷Sr/⁸⁶Sr profile (Nana Yobo et al., 2021) and the return to baseline carbonate δ^{53} Cr values.

In contrast, Wang et al. (2016) suggested that changes in the relative importance of certain Cr sinks with differences in implied isotope fractionation are driving the negative δ^{53} Cr excursion. The motivation for the sink-change hypothesis is credited to the study of Reinhard et al. (2014) who concluded that euxinic marine sinks do not fractionate seawater Cr isotopes. The warrant for this claim was questioned by Scheiderich et al. (2015) who observed that the authors did not measure seawater δ^{53} Cr values in Cariaco Basin waters, thus making any interpretation of fractionation of Cr isotopes removed by euxinic marine sediments to be speculative in the light of the variability in seawater δ^{53} Cr values. Instead, using a combination of literature data on Cr, Sr, and Os isotopes, and Os concentrations with new Cr isotope data from this study, combined with discussion of the role played by water column anoxia in the dispersal of dissolved Cr(III) species in the oceans, we build the case for major perturbations of the ocean Cr cycle centered around LIP volcanism in the geological past, which we think is more important than climate change (Jenkyns et al., 2017) or sink-switching (Wang et al., 2016) during OAE 2.

5.2. On the significance of reaching igneous-inventory values in the peak interval of the negative $\delta^{53}\text{Cr}$ excursion

There is growing evidence that *syn*-depositional processes are responsible for the bulk of Cr accumulation in marine carbonate sediments, meaning that only a small fraction of the seawater-derived Cr was acquired when the carbonate minerals were first formed by their biological progenitors (Holmden et al., 2016; Remmelzwaal et al., 2019). For example, shallow water carbonate sediments from the Caribbean Sea are 7–67 times more concentrated

in Cr, relative to Ca, than seawater (Holmden et al., 2016). High Cr concentrations in bank-top carbonate sediments are also observed in the Bahamas (Pereira et al., 2016; Farkaš et al., 2018; Klaebe et al., 2021; Wang et al., 2021). In another study, core-top foraminifera record Cr concentrations that are two orders of magnitude higher than specimens collected from plankton tows and sediment traps, or grown in culture experiments (Remmelzwaal et al., 2019). The post-depositional enrichment of Cr by marine carbonates may involve several processes, including: (1) Cr(VI) reduction to particle reactive Cr(III) in oxygendeficient pore-fluids, (2) Cr(VI) adsorption to carbonate grains (Albadarin et al., 2012; Correa et al., 2013), (3) Cr(III) adhering to exports of particulate organic matter (Semeniuk et al., 2016), and (4) incorporation of Cr(VI) into calcite cement (Füger et al., 2019). Considering the speciation of Cr associated with these mechanisms, carbonate sediments are expected to contain both Cr(VI) and Cr(III) of seawater origin. Moreover, it is generally observed that the Cr in marine carbonate sediment is isotopically lighter than local seawater sources (discussed in detail in Section 5.6; Holmden et al., 2016; Farkaš et al., 2018; Klaebe et al., 2021; Wang et al., 2021), indicating that one or more of mechanisms of post-depositional uptake of Cr by marine carbonate sediment fractionates seawater Cr isotopes (see also, Remmelzwaal et al., 2019).

Central to this theme of post-depositional enrichment of Cr in marine carbonate sediments is the recognition that carbonate bioclasts consist of micrometer-scale crystallites of calcite and/or aragonite within an organic matter matrix. Microbial respiration of the organic matrix may generate oxygen depletion in the intercrystalline spaces of the bioclasts even in settings where the sedimentary pore fluids are oxygenated or intermittently oxygenated, making the interiors of bioclastic particles feasible locations for reduction of Cr(VI) to Cr(III). Metastable aragonite and high Mg-calcite are susceptible to dissolution and reprecipitation reactions, as demonstrated by the presence of tiny carbonate overgrowths on biologically produced microcrystals (Hover et al., 2001). Remmelzwaal et al. (2019) further showed that post-depositional uptake of Cr is spatially associated with the elevated Fe and Mn concentrations in foraminifera. A subset of the examined foraminifera showed trace metal enrichment towards the rims, implying metal diffusion into the tests from the surrounding pore fluids. Other tests showed more spatially heterogenous distributions of Cr and Fe, thus revealing differences in the pathways by which these metals entered the tests. Indeed, higher resolution nanoSIMS mapping showed elevated concentrations of Cr and Fe associated with primary organic sheets which may have served as conduits for pore fluids to enter the tests (Remmelzwaal et al., 2019).

Considering the varied processes that may govern post-depositional enrichment (and diagenesis) of seawater derived Cr in marine carbonate sediments with Cr in both oxidation states, it is reasonable to question the extent to which changes in depositional facies can influence stratigraphic records of δ^{53} Cr values in marine carbonate sediments. Although more work is needed to fully address this question, we give several reasons below why we think

it is unlikely that facies-dependent changes in depositional enrichment processes or diagenesis are the cause of the low δ^{53} Cr values in the Iona-1 core. First, similarly low peak-minimum values are observed in the Portland #1 core (Fig. 4) in stratigraphically equivalent intervals despite being located 1200 km apart (Fig. 2). Second, previous explanations for the lowering of Cr isotopes in carbonate sediments relative to seawater, including Cr(VI) reduction (e.g., Holmden et al., 2016), changing coordination of Cr (VI) with pH (Füger et al., 2019), greater meteoric diagenesis (Wang et al., 2021), or changes in the mixing proportions of autochthonous (pelagic) vs. allocthonous (platform) carbonate sediment (Klaebe et al., 2021) are not applicable to the depositional setting of the study core. The Iona-1 carbonates are diagenetically stable low magnesium calcite deposits from planktic calcifiers and were never exposed to subaerial conditions. The source mixing hypothesis is only applicable to periplatform sediments, such as those draping the margins of the shallow water Bahamas Platform where exported aragonitic sediment from the platform top (with δ^{53} Cr values of $\sim 0.8\%$) mixes with pelagic calcite sediment (with δ^{53} Cr values of $\sim 0.6\%$). The depositional setting of the Iona-1 core, in the Maverick Basin, is situated squarely in the pelagic realm. Moreover, the late Cenomanian transgression drove the shoreline further away from the study setting near the onset of OAE 2, decreasing

the delivery of siliciclastic material by rivers and dust (e.g., Minisini et al., 2018).

Returning to the question of whether the attainment of igneous inventory values in the WIS is meaningful or a coincidence depends on redox transformations (or lack thereof) of volcanically derived Cr(III), and the speciation of Cr removed by carbonate sediments in the WIS during OAE 2 (Segment C in the Iona-1 core). In the absence of oxidation of hydrothermal Cr(III) to Cr(VI), the igneous inventory signature would be imparted directly to the sediments where the hydrothermal Cr(III) is removed, assuming that there is little or no isotopic fractionation of Cr (III) during particle scavenging. Alternatively, if hydrothermal Cr(III) is partially oxidized, then heavy isotopes of Cr would be preferentially transferred to the pool of seawater Cr(VI) (Bauer et al., 2019; Miletto et al., 2021) leaving the residual pool of hydrothermal Cr(III) with δ^{53} Cr values below the igneous inventory, which is not observed in this study or the two other published studies. On the other hand, if the oxidation of hydrothermal Cr(III) is quantitative, then the igneous inventory signature will be directly transferred to Cr(VI) and hydrothermal and continental weathering inputs would mix with each other in the soluble Cr(VI) pool in the oceans, obscuring their specific sources. Due to the greater solubility of Cr(VI) compared to Cr(III). and efficient mixing by the ocean circulation regime, this

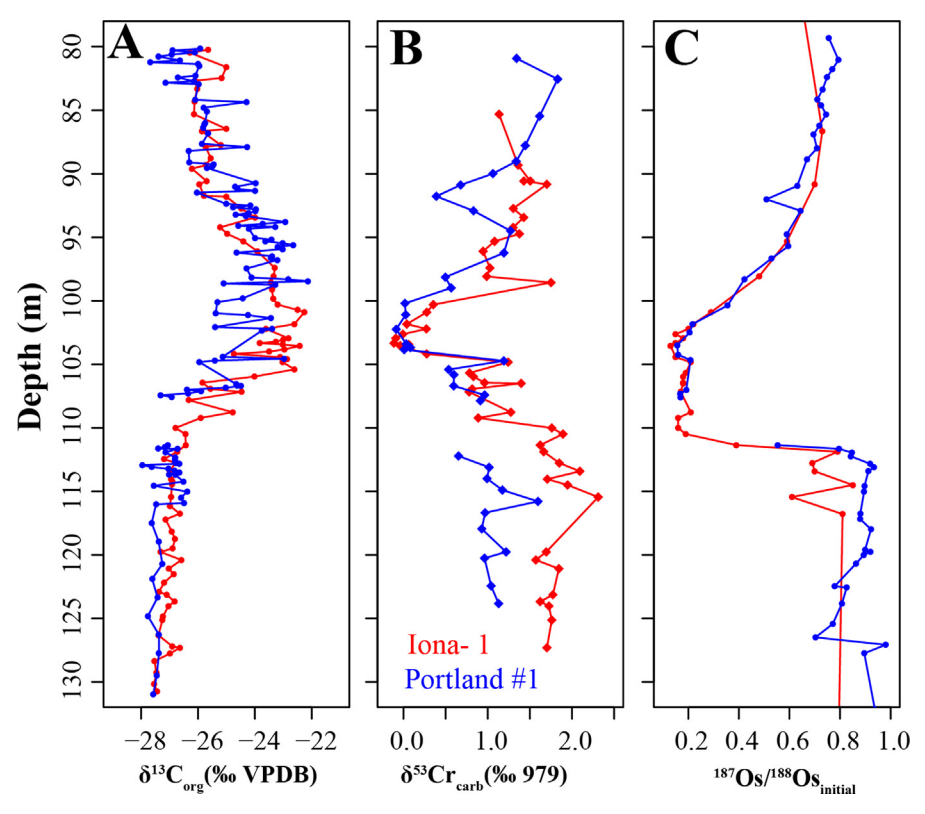


Fig. 4. Stratigraphic comparison of δ^{53} Cr values from the Iona-1 and Portland #1 cores. The stratigraphic height of the Portland #1 core is adjusted to account for the \sim 60 kyr hiatus (Jones et al., 2020) at the onset of OAE 2 in the Portland core. Data from the Portland #1 core are previously published: δ^{13} C of organic carbon (Sageman et al., 2006), 187 Os/ 188 Os (Du Vivier et al., 2014), and Al-corrected δ^{53} Cr (Holmden et al., 2016). The data from the Iona-1 core include δ^{13} C (Eldrett et al., 2014), 187 Os/ 188 Os (Sullivan et al., 2020), and carbonate δ^{53} Cr (this study).

would lower the δ^{53} Cr value of the entire ocean Cr reservoir. The oceanic residence time of Cr(VI) is estimated to be ~9000–39,000 years (Campbell and Yeats, 1981; Reinhard et al., 2014), longer than the ocean mixing time of about 1000 years. Meanwhile, the residence time for Cr (III) in oxygenated seawater is on the order of months to years, with local variation depending on oxidant type and availability and the stabilizing effects of different organic complexes (Cranston and Murray, 1978; Schroeder and Lee, 1975; Emerson et al., 1979; Pettine and Millero, 1990).

Because the solubility of Cr(III) is less than that of Cr(VI) in oxygenated seawater, it might be expected that carbonate sediment with hydrothermal Cr(III) signatures decrease with distance away from the volcanic source. On the other hand, if it were necessary to first oxidize hydrothermal Cr(III) to Cr(VI) before it could be transported away from the igneous source, then the observation that carbonate $\delta^{53}Cr$ values overlap with the igneous source would indicate a coincidence, with positive isotope fractionation associated with partial Cr(III) oxidation matching negative isotope fractionations associated with Cr(VI) reduction and uptake of Cr(III) during post-depositional enrichment processes, as described earlier in this section.

The consequences of all of these plausible sources of post-depositional uptake-related fractionation of Cr isotopes by marine sediments leads us to conclude that the simplest explanation for peak-minimum carbonate δ^{53} Cr values with the signature of the igneous inventory is for hydrothermally sourced Cr(III) to be delivered to the WIS without changing its oxidation state (Holmden et al., 2016). This further implies that intermediate and deep waters along transport paths between the LIP eruption site in the eastern Pacific and sites throughout the proto-North Atlantic basin were anoxic, as this would inhibit the partial oxidation to Cr(III) to Cr(VI) that is necessary for Cr(III) to maintain its hydrothermal δ^{53} Cr signature (or else the oxidation occurred without fractionation by an unknown mechanism). In addition, widespread anoxic conditions favor the abundance of dissolved organic ligands that may complex with Cr(III) to increase its solubility during transport. Of course, hydrothermally sourced Cr could also mix into the oceans in both oxidation states. These processes and pathways of hydrothermal Cr addition to the oceans are further considered in the next section.

5.3. A model for the negative δ^{53} Cr excursion during OAE 2

A conceptual model is proposed to explain the two-step decrease in $\delta^{53} \text{Cr}$ values recorded in the Iona-1 core during OAE 2 in the context of its relative proximity location to the Caribbean and High Arctic LIPs and the nutrient trap behavior of the proto-North Atlantic Ocean. In this interpretation, which builds on the model of Holmden et al. (2016), ingress of Cr(III) of hydrothermal origin is upwelled into the epicontinental WIS from oxygen-deficient deep waters of the proto-North Atlantic. As the oxygen-deficient waters circulated into the shallow and more oxygenated waters of the WIS, hydrothermal Cr(III) was slowly scavenged by particles and exported to the sediment, where it mixed with post-depositional uptake fluxes of

Cr(VI) and Cr(III) of seawater origin, i.e., Cr(VI) or Cr(III) produced by reduction of Cr(VI). Only during the youngest and final pulse of volcanism did the balance shift to predominantly hydrothermal sources of Cr(III) removal into the sediment in the south-central and southern region of the WIS. This implies a very low oceanic inventory of Cr(VI) at this time, or higher supply rates of hydrothermal Cr(III), though neither situation is mutually exclusive.

The model accounts for the observation that the peak-negative δ^{53} Cr values recorded by marine carbonates overlap (but do not dip below) the igneous inventory value during OAE 2. This can be attributed to Cr(III) of hydrothermal origin mixing into the WIS and dominating the Cr inventory of its waters, including the lack of isotope fractionation during post-depositional uptake of Cr(III) into marine carbonate sediments. It also accounts for the higher concentration of Cr and other trace metals of basaltic affinity in the peak-excursion interval. Moreover, this model is applicable to the record in the Portland #1 core where it was first used by Holmden et al. (2016) to explain the negative excursion in inferred seawater δ^{53} Cr values in that location, but where the hiatus in sedimentation near the onset of OAE 2 conceals the strong link with volcanism found in this study of the Iona-1 core (Fig. 4).

The model presented here can also explain why the negative δ^{53} Cr excursion recorded in the continental margin upwelling center at Demerara Rise did not reach the igneous inventory value during OAE 2. In this oxygen depleted zone (ODZ), high productivity in surface waters resulted in high rates of Cr(VI) reduction, creating locally high and sustainable concentrations of seawater-derived Cr(III) that could mix with and dilute the advected fluxes of hydrothermal Cr(III) drawn into the ODZ at depth by the quasi-estuarine circulation system of the proto-North Atlantic. Scavenging and removal of Cr(III) by particles transferred the δ^{53} Cr value of this mixed pool of Cr(III), which was higher than that of the igneous inventory, to the sediments, thus accounting for the smaller negative δ^{53} Cr excursion during OAE 2 in this setting. The lower sedimentary Cr concentrations in the excursion interval in this setting are consistent with the interpretation of a smaller oceanic inventory of Cr(VI) during OAE 2 (Wang et al., 2016). In other words, the input of hydrothermal Cr(III) to this setting was large enough to decrease the $\delta^{53}Cr$ values during OAE 2 in this setting, but not large enough to mask the effect that decreased oceanic inventories of Cr(VI) would have on local scale production rates of Cr(III).

Assuming mixing between hydrothermal Cr(III) with a $\delta^{53} Cr$ of -0.1% and seawater Cr(VI) with minimum $\delta^{53} Cr$ values of $\sim 1.5\%$ in the WIS and $\sim 1.2\%$ in the proto-North Atlantic (estimated from the measured pre-excursion background values), simple mass balance calculations indicate that just $\sim \!\! 4\%$ of the Cr deposited in the peakminimum interval of the $\delta^{53} Cr$ excursion in the study setting in the WIS was from seawater-derived Cr(VI), compared to 50% at Demerara Rise. The approximately tenfold difference in the estimated contributions of seawater Cr(VI) and hydrothermal Cr(III) is more reliable than the values themselves, as the true $\delta^{53} Cr$ values for the seawater Cr(VI) pools in each setting during OAE 2 are difficult to

estimate due to uncertainty in isotope fractionation factors and mechanisms affecting removal of Cr isotopes into marine sediments.

5.4. A Cr isotope proxy for submarine volcanism?

Chromium isotopes have been promoted as a tracer for the Precambrian oxygenation of Earth surface environments on the basis that the initial oxygenation of the atmosphere caused δ^{53} Cr values in marine sediment to deviate from those of the upper continental crust (Crowe et al., 2013; Frei et al., 2009; Planavsky et al., 2014). Chromium isotopes also have potential to identify periods of ocean de-oxygenation in the more recent geological past. But as this study and two others (Holmden et al., 2016; Wang et al., 2016) have shown, δ^{53} Cr values do not respond to de-oxygenation as expected. As discussed above, the study locations inhabit the nutrient trap configuration of the proto-North Atlantic basin and its surrounding epicontinental seas, where new inputs of hydrothermal Cr(III) may have affected local/regional budgets of Cr more strongly than other oceanic regions. Therefore the possibility remains that marine sediments may record a positive excursion elsewhere in the world's oceans during OAE 2, but only if LIP-derived hydrothermal Cr(III) was scavenged and removed before it could circulate to those regions (Holmden et al., 2016), and the amount of hydrothermal Cr(III) oxidized to Cr(VI) was small in comparison to continental weathering inputs of Cr.

On the other hand, massive episodes of submarine volcanism may be a more common driver of ocean de-oxygenation than previously believed, making the Cr isotope proxy challenging to implement and interpret with confidence. In fact, there are no indications that δ^{53} Cr values in modern marine sediments uniquely track dissolved seawater O₂ concentrations (Moos and Boyle, 2019; Goring-Harford et al., 2018; Janssen et al., 2020; Nasemann et al., 2020; Huang et al., 2021; Janssen et al., 2021). The spatial variability in seawater δ^{53} Cr values is primarily controlled by the interconversions of Cr(VI) and Cr (III) that occur in relation to the biological pump, and by mixing of isotopically distinct water masses by ocean currents (Scheiderich et al., 2015; Janssen et al., 2020, 2021). The biological pump operates in both oxygenated and deoxygenated regions of the oceans. Shallow marine carbonate sediments deposited in oxygenated waters of the Caribbean and Bahamas record the same range of δ^{53} Cr values $(\pm 0.6 \text{ to } \pm 0.7\%)$ (Bonnand et al., 2013) as recently deposited sediments beneath the Peruvian ODZ (+0.4 to +0.8%) (Gueguen et al., 2016; Bruggmann et al., 2019) and euxinic bottom waters of the Cariacao Basin (+0.5%) to +0.7%; Reinhard et al., 2014).

There is also no correlation between seawater $[Cr]_T$, $\delta^{53}Cr$ and dissolved oxygen in oxygen minimum zones (OMZs) (Goring-Harford et al., 2018; Moos and Boyle, 2019) or ODZs (Nasemann et al., 2020; Huang et al., 2021). Instead, strong correlations exist between total dissolved Cr and $\delta^{53}Cr$ values in seawater on a global scale (e.g., Scheiderich et al., 2015), and nutrient distributions

(N, P and Si) on the more local/regional scale (Campbell and Yeats, 1981; Jeandel and Minster, 1987), lending support for the use of Cr isotopes in water-mass tracing, or as a carbon export proxy (Scheiderich et al., 2015; Janssen et al., 2020). Variations in δ^{53} Cr values in marine sediments accumulating beneath ODZs may indirectly track climate or ocean circulation-driven changes in the area of oxygen-depleted waters (and underlying sediments), but only because local/regional changes in oxygen utilization positively correlate with similar scale changes in Cr (III) exports. For example, a strong expansion of ODZs in one or more oceanic regions could lead to a global increase in seawater δ^{53} Cr values as the local effects of increased C exports in ODZs is propagated via ocean circulation. And as indicated above, such positive shifts might still be found in other regions of the oceans during OAE 2. However, given the apparently widespread negative shift in inferred seawater δ^{53} Cr in the proto-North Atlantic region during OAE 2, the application of Cr isotopes as a proxy for submarine volcanism also warrants consideration when interpreting Cr isotope records of marine sediments in the geological past.

Though it is generally agreed that hydrothermal contributions to the Cr budget of the well oxygenated modern ocean are negligible due to scavenging and removal of hydrothermal Cr(III) by Fe-oxyhydroxides and Fesulfides at ridge-crest hydrothermal vents (Jeandel and Minster, 1984), there is still evidence that some hydrothermal Cr(III) escapes this fate in some locations. For example, Sander and Koschinsky (2000) reported high dissolved Cr(III) concentrations in the Fiji Basin, which they attributed to seepages of low temperature fluids from the basaltic sea floor and higher temperature fluids from nearby hydrothermal vents. They credited Cr(III) stability in these oxygenated waters to organic complexation, noting the presence of dense bacterial mats and hydrothermal fauna on the seafloor as plausible sources of organic matter. In another study, basalt-seawater interactions along the coast of Hawaii also show enrichments in dissolved trace metals (Fe, Mn, Ni, Co, Cu, and Zn) in the areas where lavas enter the oceans (Hawco et al., 2020). These are the same metals that are commonly enriched with Cr in marine carbonate deposited during OAE 2 (e.g., Orth et al., 1993; Sinton and Duncan, 1997; Snow et al., 2005; Eldrett et al., 2014, 2015a; and Jenkyns et al., 2017) though Cr was not itself measured in the Hawaiian study. In seawater near the Lesser Antilles Island Arc where mantle-derived ³He has been reported (Polyak et al., 1992), dissolved Cr (III) concentrations correlate positively with dissolved Zn concentrations, which Sander et al. (2003) attributed to local hydrothermal inputs. Off the coast of Granada, seawater profiles sampled between 2 and 50 m also record strong correlations ($r^2 = 0.96$) between dissolved Cr(III) and Zn attributed to the release of these metals by submarine hot springs that are common in the region (Johnson and Cronan, 2001; Halbach et al., 2001). The correlation between Cr(III) and Zn is also found in deeper water profiles off the island of Dominica (800-1200 m), and between 25 and 150 m in waters off the coast of St. Lucia (Johnson and Cronan, 2001), further supporting the expectation that hydrothermally derived metals abundances are expected to covary.

The evidence for hydrothermal Cr(III) in the modern oceans presage the much larger inputs that would occur in the geological past during periods of more pervasively deoxygenated oceans, such as during the Precambrian when atmospheric oxygen levels had not yet risen to modern levels, or at any time in Earth history when submarine volcanic activity was high. Volcanically active marginal or rifted marine basins are prime locations where shifts to lower seawater-derived δ^{53} Cr values may be evident in settings with locally elevated levels of submarine volcanism. driving carbonate δ^{53} Cr values towards, but not below, the igneous inventory minimum. Additional supporting evidence for submarine volcanism from other trace metals and their isotopes, e.g., Fe, Ni and Zn isotopes, trace metal abundance anomalies of basaltic affinity, Os concentrations, and Os and Sr isotopes could be used together to strengthen suspected connections between submarine volcanism and negative Cr isotope excursions, particularly in cases where the peak minimum values reach the igneous inventory value.

Because hydrothermal activity delivers Cr to the oceans with a low and uniform δ^{53} Cr value compared to oxidativeweathering inputs of Cr from the continental crust, seawater δ^{53} Cr is predicted to decrease during submarine eruptions of LIPs, but by how much depends on the balance of the continental and hydrothermal input fluxes of Cr to the oceans, the fraction of the hydrothermal Cr(III) flux that is oxidized to Cr(VI), and the mechanism and fractionation factor accompanying this oxidation. Oxidation of Cr (III) could occur in contact with oxygenated seawater along the margins of the anoxic plumes where high Mn(II) concentrations would encourage formation of nanoparticulate Mn(III-IV) oxides which are strong oxidizing agents of Cr (III) (Eary and Rai, 1987). On the other hand, high Fe(II) concentrations in the plume would promote backreduction of Cr(VI) to Cr(III), as ferrous iron is a strong reducing agent of Cr(VI) (Døssing et al., 2011). Literature studies show that if oxidation-reduction is not quantitative, the reactions tend to favor the accumulation of heavy isotopes in Cr(VI) (Bauer et al., 2019; Miletto et al., 2021).

It is therefore possible that the δ^{53} Cr value of seawater decreased everywhere in the oceans during OAE 2 if sufficiently large quantities of hydrothermal Cr(III) were oxidized to Cr(VI) and the fractionation factor was small. If this can be demonstrated with δ^{53} Cr records from the Pacific, it would further undermine the utility of δ^{53} Cr as a paleoredox proxy during OAE 2, while supporting its potential as a proxy for submarine eruptions of LIPs. Indeed, there is growing evidence that eruptions of other LIPs may have occurred during OAE 2, such as the High Arctic LIP in the Arctic Ocean (Schröder-Adams et al., 2019), and that these may have also contributed to locally lowering the δ⁵³Cr value of seawater and marine sediments in other regions of the oceans during OAE 2. These additional sources of hydrothermal Cr(III), if subsequently oxidized to Cr(VI), may have likewise contributed to the hypothesized global decline in the δ^{53} Cr value of the ocean Cr (VI) reservoir as well. On the other hand, if the Caribbean

LIP were the main source of hydrothermal Cr(III) to the oceans during OAE 2, the proto-North Atlantic may have trapped and removed much of it before it could be oxidized and thoroughly mixed by the ocean circulation regime.

5.5. Climate change did not cause the negative $\delta^{53} Cr$ excursion during OAE 2

Jenkyns et al. (2017) tied trace metal anomalies in the Plenus Marls in the English Chalk to changes in climate rather than volcanism. Many of these metals, including Cr. are enriched at the same stratigraphic interval as the second step-shift to lower δ^{53} Cr values in the Iona-1 core, and the main shift in Portland #1 core, which is the peak negative shift that reaches igneous inventory values (Segment C, Figs. 3, 4). Jenkyns et al. (2017) suggested that the correlation of this stratigraphic interval with the PCE might imply a global-scale release of redox sensitive metals from formerly anoxic marine sediment. Jenkyns et al. (2017) further emphasized that their sediment release model for metals does not require an additional volcanic or hydrothermal input of Cr during OAE 2. They assumed that the Cr sequestered by anoxic marine sediments occurred during an earlier phase of OAE 2 and was originally Cr(VI) of seawater origin.

There are major problems with this hypothesis. First, it conflicts with volcanic proxy indicators (Os, Sr isotopes) (Sullivan et al., 2020; Nana Yobo et al., 2021) of increased (not decreased) volcanism during parts of the PCE in records from the WIS, and Nd isotope records from the Anglo-Paris Basin (Zheng et al., 2013). Second, an evaluation of the origins of the PCE by O'Connor et al. (2020) concluded that cooling was more likely of regional than global significance. Another problem is that the euxinic marine sediments deposited at Demerera Rise, which are an example of the source of trace metals proposed to be oxidized and released to seawater during the PCE, have higher δ^{53} Cr values than the PCE-equivalent strata in the WIS. Therefore, an endmember source of Cr with even lower δ^{53} Cr is required. When it is further considered that oxidation of Cr(III) in sediments is unlikely to be quantitative, which will promote the release Cr(VI) to seawater that is higher in δ^{53} Cr than the sediment source (Bauer et al., 2019; Miletto et al., 2021), it is clear that sediment release of Cr cannot explain the peak negative δ^{53} Cr values in the excursion interval during OAE 2. Even in sediments where hydrothermal Cr(III) may have accumulated, partial oxidation of Cr(III) would still favor the release of the heavy Cr isotope.

Many other trace metals are commonly enriched in sediments deposited during OAE 2, and most of them have two or more isotopes that could be used to determine their origins. For example, anomalous concentrations of Zn occur in the same stratigraphic intervals as Cr in the Iona core and Gongzha section in Southern Tibet, and the shift to negative δ^{66} Zn values has been interpreted to reflect new inputs of LIP-derived hydrothermal Zn to the oceans during OAE 2 (Sweere et al., 2020; Chen et al., 2021). More work on transition metal isotopes like Zn that are insensitive to environmental redox conditions could help

to disentangle sedimentary and volcanic source of Cr to the oceans during OAE 2.

5.6. Further notes on the speciation of Cr in marine carbonate sediment and estimates of seawater $\delta^{53} Cr$ values before and after OAE 2

The proposed interpretive model for post-depositional uptake of Cr by marine carbonate sediments includes transformations and fractionations of Cr(VI) and Cr(III) sources that separately and together could impact the Cr isotope values preserved in marine carbonates. Here we consider the proportions of Cr(VI) and Cr(III) in the sediments. The mass balance calculation from section 5.2 indicates that 96% of the Cr in the carbonates with the lowest δ^{53} Cr values may be attributed to the removal of hydrothermal Cr (III) from seawater in the Iona-1 setting. It follows that the speciation of Cr released by the acetic acid attack, which was employed to dissolve carbonate minerals, must be predominantly Cr(III) if the model presented here is correct, which also has implications for how Cr(III) is immobilized and ultimately preserved in carbonate sediments.

Observations suggest that Cr(III) is associated with particles and therefore has a high likelihood of being incorporated into carbonate sediments. The association of Cr(III) with phytoplankton is initiated in the water column as shown by growth experiments using artificial seawater doped with environmentally relevant concentrations of Cr (VI) and radioactive ⁵¹Cr as a tracer (Semeniuk et al., 2016). More Cr was found on the outside of the phytoplankton cells than within the cytoplasm of the cells, even when the plankton were grown in seawater containing only Cr(VI) species. This implies that reduction of Cr(VI) occurred during phytoplankton growth. In subsequent experiments where Cr(III) was directly added to the artificial seawater, more Cr was adsorbed to cell surfaces. The further addition of Fe to the culture medium resulted in more uptake of Cr(III) by the plankton due to the adsorption/formation of amorphous Fe-oxyhydroxides on the cell surfaces, which created additional exchange sites for the adsorption of Cr(III) (Semeniuk et al., 2016). These experimental results demonstrate the affinity of various types of phytoplankton for the adsorption of Cr(III) and are relevant for coccolithophorids, one of the main bioclastic constituents of pelagic marine carbonate in the study core. Coccoliths (plates or scales of low magnesium calcite) form intracellularly within Golgi vesicles (Outka and Williams, 1971). To reach the outside of the cell the calcite plate must be extruded through the cell wall. And as the outer cell wall captures most of the seawater derived Cr(III) found in both mineralized and unmineralized phytoplankton studied in the growth experiments (Semeniuk et al., 2016), the Cr delivered to the sediments by the pelagic rain of coccoliths is most likely Cr(III) that is adsorbed to the cells, rather than Cr(VI) that co-precipitated with the calcite.

Chromium (III) availability in surface waters is normally tied to Cr(VI) reduction, which is episodic and linked to phytoplankton blooms (Connelly et al., 2006). During OAE 2, when elevated sources of Cr(III) of hydrothermal origin were available for scavenging, the locally produced

Cr(III) from reduction of Cr(VI) would be diluted. Particles settling through the water column, including calcareous test and coccoliths, would scavenge Cr(III) and transfer it to the sediment. In the sediment, Cr(III) could then be mobilized from the surfaces of the particles and transferred into carbonate phases during *syn*-depositional diagenesis, analogous to the incorporation of trivalent REE into calcite (Marques Fernandes et al., 2008) with the appropriate charge-balancing substitution of Ca for a monovalent cation. Cr(III) could also translocate along with reduced iron into carbonate bioclasts where it could be immobilized by Fe-oxyhydroxides (Remmelzwaal et al., 2019).

Scavenging of Cr(III) by sinking particles represents one facet of the post-depositional uptake flux of Cr(III) into marine sediments. Cr(VI) may also diffuse into pore waters from bottom waters, and then reduced to Cr(III) in the anoxic interiors of bioclastic grains, as discussed above. There is also the spatial variability in the pore fluid redox conditions to consider, especially in shallow water sediments prone to disturbances by waves, currents, and mixing by bioturbating organisms. Moreover, Cr(VI) is also known to adsorb to carbonate mineral surfaces (Albadarin et al., 2012). Sediments that remain in contact with seawater for longer periods of time before they are buried should acquire higher Cr concentrations (Holmden et al., 2016; Remmelzwaal et al., 2019). Ultimately, Cr (VI) and Cr(III) may both become incorporated into new carbonate overgrowths and cements regardless of their sources and original oxidation states. The key point is that an acetic acid leach of a carbonate bioclast or sediment will release more Cr than that which only resides in the lattice framework of carbonate minerals.

Though the spectrum of possible mechanisms controlling post-depositional uptake and fractionation of seawater-derived Cr into carbonate sediments are potentially large, the similarity in Cr concentrations between modern and ancient marine carbonates suggests that there are dominant pathways by which carbonate sediments accumulate seawater-derived Cr that are consistent in space and time. To illustrate, the [Cr] in pelagic marine carbonate sediments deposited before and after OAE 2 in the WIS range between 0.6 and 16 ppm (Table 1 and Holmden et al., 2016), which fall within the range of Cr concentrations in shallow-water carbonate sediments in the Caribbean Sea (2.9-9.2 ppm) (Holmden et al., 2016) and Bahamas platform (1.3-3.9 ppm) (Klaebe et al., 2021). The range of Cr concentrations in buried carbonate sediments draping the margins of the Bahamas platform (Klaebe et al., 2021) record higher Cr concentrations (0.9) to 19 ppm) but the median Cr concentration of 6.6 ppm falls in the range of the other reported values. Though the range may seem to be potentially significant at first glance, it is worth remembering that there is 7-100 times more Cr than Ca in marine carbonates than seawater, which makes the approximately ten times range of Cr concentration in modern marine carbonates seem small by comparison. This suggests that similar mechanisms are controlling postdepositional uptake of Cr into marine carbonate sediments in different settings.

Table 1 Chromium concentration and isotope data from carbonate fractions of the Iona-1 Core.

Depth	Carb Weight fraction ^a	Cr ID (ppm) ^b	Al (ppm) ^c	Ti (ppm) ^c	$\delta^{53}Cr^{\textcolor{red}{d}}$	2se ^e	Corrected F	or Al		Corrected F	or Ti	
							δ ⁵³ Cr corr.	Cr carb (ppm)	Detrital fract.	δ^{53} Cr corr.	Cr carb (ppm)	Detrital fract
85.31	0.95	1.25	75	0.01	1.10	0.11	1.13	1.22	0.03	1.10	1.25	0.00
89.32	0.42	3.32	80	0.00	1.32	0.03	1.34	3.28	0.01	1.32	3.32	0.00
90.57	0.59	2.07	146	0.13	1.41	0.02	1.47	2.00	0.03	1.41	2.06	0.00
90.57	0.44	5.32	44	0.00	1.41	0.02	1.42	5.30	0.00	1.41	5.32	0.00
90.83	0.17	1.93	35	0.00	1.61	0.02	1.62	1.92	0.01	1.61	1.93	0.00
92.73	0.43	1.53	359	0.30	0.93	0.05	1.06	1.36	0.11	0.93	1.53	0.00
93.44	0.32	1.64	71	0.00	1.33	0.03	1.36	1.60	0.02	1.33	1.64	0.00
94.22	0.43	1.77	58	0.03	1.25	0.06	1.27	1.74	0.02	1.25	1.77	0.00
94.73	0.37	1.70	76	0.00	1.29	0.02	1.32	1.66	0.02	1.29	1.70	0.00
95.32	0.20	1.58	44	0.00	1.00	0.01	1.02	1.55	0.01	1.00	1.58	0.00
96.10	0.59	2.29	100	0.04	0.91	0.04	0.93	2.24	0.02	0.91	2.29	0.00
97.41	0.47	2.20	73	0.00	0.99	0.03	1.01	2.17	0.02	0.99	2.20	0.00
98.08	0.36	1.01	97	0.00	0.85	0.03	0.89	0.96	0.05	0.85	1.01	0.00
98.56	0.41	4.00	61	0.06	1.72	0.04	1.73	3.97	0.01	1.72	4.00	0.00
100.30	0.32	5.24	183	0.09	0.33	0.06	0.34	5.15	0.02	0.33	5.24	0.00
100.90	0.51	1.98	236	0.83	0.23	0.02	0.25	1.86	0.06	0.23	1.97	0.01
101.83	0.25	2.61	50	0.25	0.03	0.03	0.03	4.01	0.01	0.03	4.03	0.00
102.21	0.33	4.03	334	1.25	0.22	0.02	0.23	5.59	0.03	0.23	5.73	0.00
102.63	0.19	5.75	132	0.00	-0.01	0.02	-0.01	5.68	0.01	-0.01	5.75	0.00
102.95	0.29	8.01	276	0.00	-0.09	0.07	-0.09	7.88	0.02	-0.09	8.01	0.00
103.33	0.15	15.84	1261	0.00	-0.12	0.02	-0.11	15.23	0.04	-0.12	15.84	0.00
103.44	0.63	7.08	37	0.12	0.06	0.02	0.06	7.06	0.00	0.06	7.08	0.00
103.54	0.19	6.56	105	0.00	-0.04	0.02	-0.04	6.51	0.01	-0.04	6.56	0.00
104.18	0.43	2.57	54	0.05	0.26	0.14	0.27	2.54	0.01	0.26	2.57	0.00
104.83	0.50	1.44	290	0.67	0.98	0.04	1.10	1.30	0.10	0.98	1.43	0.01
105.68	0.40	1.64	73	0.00	0.74	0.02	0.75	1.60	0.02	0.74	1.64	0.00
105.96	0.42	0.81	70	0.30	0.74	0.05	0.77	0.78	0.04	0.74	0.81	0.00
106.45	0.33	3.05	254	1.10	0.83	0.03	0.87	2.93	0.04	0.84	3.04	0.00
106.50	0.45	2.60	72	0.00	1.35	0.02	1.37	2.57	0.01	1.35	2.60	0.00
106.94	0.51	0.97	152	0.03	0.68	0.11	0.74	0.90	0.08	0.68	0.97	0.00
107.17	0.55	2.02	153	0.41	0.72	0.02	0.75	1.95	0.04	0.72	2.02	0.00
108.77	0.43	0.62	111	0.29	0.99	0.09	1.10	0.57	0.09	1.00	0.62	0.01
109.22	0.45	1.59	28	0.00	0.87	0.03	0.88	1.58	0.01	0.87	1.59	0.00
110.01	0.43	4.52	31	0.00	1.75	0.03	1.75	4.50	0.00	1.75	4.52	0.00
110.49	0.43	4.29	71	0.27	1.86	0.03	1.87	4.26	0.01	1.86	4.29	0.00
111.36	0.47	5.71	115	0.25	1.59	0.05	1.60	5.65	0.01	1.59	5.70	0.00
111.88	0.36	3.42	90	0.89	1.60	0.05	1.62	3.37	0.01	1.61	3.41	0.00
112.77	0.41	3.19	167	0.00	1.73	0.03	1.78	3.11	0.03	1.73	3.19	0.00
113.42	0.21	2.71	55	0.00	1.99	0.02	2.01	2.68	0.01	1.99	2.71	0.00
114.04	0.65	2.00	73	0.09	1.66	0.03	1.69	1.96	0.02	1.66	2.00	0.00
114.50	0.21	4.30	50	0.00	1.93	0.04	1.93	4.27	0.00	1.93	4.30	0.00
115.45	0.41	1.49	305	0.31	1.72	0.02	1.92	1.34	0.10	1.73	1.48	0.00

19.77 0.49 4.37 248 0.56 1.59 0.02 1.64 4.25 0.03 1.60 4.36 0.00 20.40 0.45 3.00 28 0.41 1.55 0.11 1.56 2.99 0.00 1.56 3.00 0.00 21.09 0.44 6.82 260 0.42 1.76 0.20 1.76 6.70 0.02 1.76 6.82 0.00 23.14 0.41 4.47 617 0.55 1.47 0.02 1.47 0.07 1.47 4.46 0.00 23.68 0.54 1.87 94 0.18 1.54 0.02 1.83 0.02 1.55 1.87 0.00 24.03 0.45 1.54 0.09 1.62 3.76 0.05 1.54 3.93 0.00 25.13 0.43 0.44 0.47 1.46 0.02 1.54 4.38 0.01 1.73 4.38 0.00 25.13 <													
0.45 3.00 28 0.41 1.55 0.11 1.56 2.99 0.00 1.56 3.00 0.44 6.82 260 0.42 1.76 0.02 1.80 6.70 0.02 1.76 6.82 0.41 4.47 617 0.55 1.47 0.02 1.83 0.07 1.47 4.46 0.54 1.87 94 0.18 1.54 0.02 1.58 1.83 0.02 1.55 1.87 0.45 3.93 373 0.45 1.54 0.09 1.62 3.76 0.05 1.54 3.93 0.43 4.38 59 0.00 1.73 0.04 1.74 4.35 0.06 1.46 3.68 42 0.47 1.46 0.02 1.55 3.48 0.06 1.46 3.68	19.77	0.49	4.37	248	0.56	1.59	0.02	1.64	4.25	0.03	1.60	4.36	0.00
0.44 6.82 260 0.42 1.76 0.02 1.80 6.70 0.02 1.76 6.82 0.41 4.47 617 0.55 1.47 0.02 1.58 4.17 0.07 1.47 4.46 0.54 1.87 0.18 1.54 0.02 1.58 1.83 0.02 1.55 1.87 0.45 1.84 0.09 1.62 3.76 0.05 1.54 3.93 0.43 4.38 59 0.00 1.73 0.04 1.74 4.35 0.01 1.73 4.38 0.42 1.36 0.02 1.55 3.48 0.06 1.46 3.68 9.06	20.40	0.45	3.00	28	0.41	1.55	0.11	1.56	2.99	0.00	1.56	3.00	0.00
0.41 4.47 617 0.55 1.47 0.02 1.58 4.17 0.07 1.47 4.46 0.54 1.87 0.18 1.54 0.02 1.58 1.83 0.02 1.55 1.87 0.45 1.84 0.09 1.62 3.76 0.05 1.54 3.93 0.43 4.38 59 0.00 1.73 0.04 1.74 4.35 0.01 1.73 4.38 0.42 1.36 0.07 1.55 3.48 0.06 1.46 3.68	21.09	0.44	6.82	260	0.42	1.76	0.02	1.80	6.70	0.02	1.76	6.82	0.00
0.54 1.87 94 0.18 1.54 0.02 1.83 0.02 1.55 1.87 0.45 3.93 3.74 0.09 1.62 3.76 0.05 1.54 3.93 0.43 4.38 59 0.00 1.73 0.04 1.74 4.35 0.01 1.73 4.38 0.42 3.69 434 0.47 1.46 0.02 1.55 3.48 0.06 1.46 3.68	23.14	0.41	4.47	617	0.55	1.47	0.02	1.58	4.17	0.07	1.47	4.46	0.00
0.45 3.93 373 0.45 1.54 0.09 1.62 3.76 0.05 1.54 3.93 0 0.43 4.38 59 0.00 1.73 0.04 1.74 4.35 0.01 1.73 4.38 0 0.42 3.69 434 0.47 1.46 0.02 1.55 3.48 0.06 1.46 3.68 0	23.68	0.54	1.87	94	0.18	1.54	0.02	1.58	1.83	0.02	1.55	1.87	0.00
0.43 4.38 59 0.00 1.73 0.04 1.74 4.35 0.01 1.73 4.38 () 0.42 3.69 434 0.47 1.46 0.02 1.55 3.48 0.06 1.46 3.68 ()	24.03	0.45	3.93	373	0.45	1.54	0.09	1.62	3.76	0.05	1.54	3.93	0.00
0.42 3.69 434 0.47 1.46 0.02 1.55 3.48 0.06 1.46 3.68 (25.13	0.43	4.38	59	0.00	1.73	0.04	1.74	4.35	0.01	1.73	4.38	0.00
	27.31	0.42	3.69	434	0.47	1.46	0.02	1.55	3.48	90.0	1.46	3.68	0.00

Gravimetric determinations after acidification to remove carbonate minerals. Cr concentration measured by isotope dilution thermal ionization mass spectrometry.

^c Concentration reported on a carbonate basis (i.e., the weight of residue is subtracted from the total weight of the sample)

2 s.e. is twice the standard error of the mean derived from the mass spectrometric measurements

The relatively narrow range of δ^{53} Cr values in modern marine settings with values ranging between \sim 0.6 and 0.9% (Holmden et al., 2016; Klaebe et al., 2021) suggest that fractionation effects are reproducible as well. Even the buried carbonates from the margins of the Bahamas platform with a range of potentially important early diagenetic effects to consider (Wang et al., 2021) fall in the range of carbonate sediment δ^{53} Cr values that have not been buried (0.70% \pm 0.20), except for pervasively dolomitized carbonates. The only modern locations where both seawater and carbonate sediment have been analyzed to date are in the Caribbean Sea, which Holmden et al. (2016) used to determine an apparent isotope fractionation ($\Delta\delta^{53}$ Cr_{sediment-seawater}) of -0.46% \pm 0.14 (2 σ).

As stated above, the average Cr concentrations in carbonate sediment deposited in the Iona-1 (0.5–16 ppm) and Portland # 1 (1.4-20 ppm) core settings before and after OAE 2 are typical when compared to Cr concentrations in modern carbonate sediment. In contrast, the δ^{53} Cr values are higher than modern marine carbonates, yielding $\sim +1.5\%$ (± 0.01 , 1σ) before OAE 2 and $\sim +1.1\%$ $(\pm 0.02, 1\sigma)$ after OAE 2 in the Iona-1 core, compared to ~0.6–0.9‰ in modern marine carbonates. Applying the nominal correction of -0.46% (Holmden et al., 2016) to these data produces estimates of seawater δ^{53} Cr values of $\sim +2.0\%$ before and $\sim +1.6\%$ after OAE 2 in the Iona-1 core setting. We do not apply the fractionation correction to the carbonates deposited during OAE 2 because they are interpreted as mixtures of seawater Cr(VI) to which the fractionation factor would apply, and hydrothermal Cr(III) to which it would not apply. The +2.0% estimate for seawater before OAE 2 is higher than modern seawater (+0.9 to +1.6%) (Bonnand et al., 2013, Scheiderich et al. 2015), but within the expected range for increased export fluxes of isotopically light Cr(III) into marine sediments due to increased local and/or global primary productivity. Alternatively, these higher values could reflect different pathways and mechanisms for Cr uptake and related fractionation factors. Either or both explanations could account for the 0.5% lower inferred seawater δ^{53} Cr in the Portland #1 core setting compared to the setting of the Iona-1 core (Fig. 4), in addition to uncertainties associated with the detrital correction. This could indicate differences in water mass origins between the two settings before OAE 2, consistent with greater circulation restrictions due to lower sea level, supported by faunal evidence for greater Boreal influences at this time in the south-central WIS (van Helmond et al., 2014; Eldrett et al., 2014). Circulation restriction was eased at the onset of OAE 2, which coincided with the late Cenomanian transgression (Eldrett et al., 2015a; Minisini et al., 2018).

6. CONCLUSIONS

The decrease in sedimentary δ^{53} Cr values in the proto-North Atlantic region during OAE 2 does not directly reflect the expansion and contraction of ocean anoxia, which predicts an increase in seawater δ^{53} Cr as the oceanic inventory of Cr(VI) decreases. This expectation assumes that all other fluxes and fractionation factors associated with redox changes and removal of Cr from seawater remain constant. It is proposed instead that LIP volcanism, the proposed trigger for OAE 2, generated large hydrothermal input fluxes of Cr(III) to the oceans that lowered sedimentary δ^{53} Cr values in the proto-North Atlantic region where this study and two others from the literature are focused. The lowest δ^{53} Cr values that are observed in the Iona-1 core at \sim 105 m depth, which is roughly equivalent to the lower part of the PCE recorded in the Anglo-Paris Basin, are indistinguishable from the igneous inventory value. This is interpreted as evidence that the oxidation state of hydrothermal Cr(III) was not isotopically fractionated between source and sink, implying that deep waters between the eastern Pacific and proto-North Atlantic were anoxic in the metal-enriched interval of the PCE, which contradicts hypotheses that anoxia decreased in the global ocean at this time during OAE 2.

Records of changing sedimentary δ^{53} Cr values during OAE 2 may indirectly imply local or even global redox shifts during OAE 2 but not in the interpretive framework that has been usually implemented. Instead of reflecting isotope fractionation associated with Cr reduction, these records can indirectly indicate periods of expanded marine anoxia caused by increased submarine volcanism (Sinton and Duncan, 1997), which created favorable redox conditions for the spread of organically-complexed hydrothermal Cr(III) (with igneous inventory values) away from the LIP eruption site. This in turn generated anomalously low carbonate δ^{53} Cr values in regions affected by the dispersal of hydrothermally sourced Cr(III), and anomalously high carbonate concentrations of Cr and other trace metals of basaltic affinity.

The record of Cr cycling during OAE 2 in the proto-North Atlantic and WIS is strongly influenced by its small volume (5% of the global ocean volume), its quasi-estuarine circulation, and the proximity to the eruption of the Caribbean LIP near the ocean gateway to the proto-North Atlantic in the present-day Central Americas (Trabucho Alexandre et al., 2010), and possibly the High Arctic LIP (Schröder-Adams et al., 2019; Sullivan et al., 2020). How the ocean Cr cycle responded to OAE 2 outside of the proto-North Atlantic region requires further study. Did hydrothermal Cr(III) circulate to the South Pacific during OAE 2, escaping oxidation to Cr(VI) as a result of globally extensive anoxia? What fraction of the hydrothermal Cr(III) input to the oceans was oxidized to Cr(VI)? And what effect did this have on the globally weighted average δ^{53} Cr value of the ocean Cr reservoir during OAE 2? Additional δ^{53} Cr records from other oceanic regions are needed to address these outstanding questions on the speciation, circulation, and transport of hydrothermal Cr in the oceans during OAE 2.

DECLARATION OF COMPETING INTEREST

The authors declare that they have no known competing financial interests or personal relationships that could have appeared to influence the work reported in this paper.

ACKNOWLEDGEMENTS

We thank Shell International Exploration and Production Inc. for making samples available. LNY thanks Nasreen Mosa and Jim Rosen for training and technical support in the Saskatchewan Isotope Laboratory. The manuscript was improved by suggestions of 2 anonymous reviewers. We also appreciate editorial handling by A. Zerkle. Funding for this project was made possible by National Science Foundation award EAR 1933302 to ADB, National Science Foundation award EAR 2124802 to KVL, an AAPG Grant In Aid to LNY, and NSERC Discovery grant and McLeod Chair funding to CH.

RESEARCH DATA

The measured Cr isotope data in this paper is provided in Table 1 and as a supplementary data file. All other data used are from previously published peer review paper and have been properly cited as necessary.

APPENDIX A. SUPPLEMENTARY MATERIAL

Supplementary material to this article can be found online at https://doi.org/10.1016/j.gca.2022.06.016.

REFERENCES

- Albadarin A. B., Mangwandi C., Ala' Al-Muhtase, Walker G. M., Allen S. J. and Ahmad M. N. M. (2012) Kinetics and thermodynamics of chromium ions adsorption onto low-cost dolomite adsorbent. *Chem. Eng. J.* 179, 193–202.
- Albut G., Babechuk M. G., Kleinhanns I. C., Benger M., Beukes N. J., Steinhilber B., Smith A. J. B., Kruger S. J. and Schoenberg R. (2018) Modern rather than Mesoarchaean oxidative weathering responsible for the heavy stable Cr isotopic signatures of the 2.95 Ga old Ijzermijn iron formation (South Africa). Geochim. Cosmochim. Acta 228, 157–189.
- Albut G., Kamber B. S., Bruske A., Beukes N. J., Smith A. J. B. and Schoenberg R. (2019) Modern weathering in outcrop samples versus ancient paleoredox information in drill core samples from a Mesoarchaean marine oxygen oasis in Pongola Supergroup, South Africa. Geochim. Cosmochim. Acta 265, 330–353.
- Babechuk M. G., Kleinhanns I. C. and Schoenberg R. (2017) Chromium geochemistry of the ca. 1.85Ga Flin Flon paleosol. *Geobiology* 15, 30–50.
- Babechuk M. G., Kleinhanns I. C., Reitter E. and Schoenberg R. (2018) Kinetic stable Cr isotopic fractionation between aqueous Cr(III)-Cl-H₂O complexes at 25 C: Implications for Cr(III) mobility and isotopic variations in modern and ancient natural systems. *Geochim. Cosmochim. Acta* 222, 383–405.
- Basu A., Johnson T. M. and Sanford R. A. (2014) Cr isotope fractionation factors for Cr (VI) reduction by a metabolically diverse group of bacteria. *Geochim. Cosmochim. Acta* 142, 349– 361.
- Bauer K. W., Cole D. B., Asael D., Francois R., Calvert S. E., Poulton S. W., Planavsky N. J. and Crowe S. A. (2019) Chromium isotopes in marine hydrothermal sediments. *Chem. Geol.* 529 119286.

- Berger A. and Frei B. (2014) The fate of chromium during tropical weathering: A laterite profile from Central Madagascar. Geoderma 213, 521-532.
- Bonnand P., James R. H., Parkinson I. J., Connelly D. P. and Fairchild I. J. (2013) The chromium isotopic composition of seawater and marine carbonates. *Earth Planet. Sci. Lett.* **382**, 10–20.
- Bruggmann S., Klaebe R., Paulukat C. and Frei R. (2019) Heterogeneity and incorporation of chromium isotopes in recent marine molluscs (Mytilus). *Geobiology* 17, 417–435.
- Campbell J. A. and Yeats P. A. (1981) Dissolved Cr in the northwest Atlantic Ocean. Earth Planet. Sci. Lett. 53, 427–433.
- Chen X., Sageman B. B., Yao H., Liu S., Han K., Zou Y. and Wang C. (2021) Zinc isotope evidence for paleoenvironmental changes during Cretaceous Oceanic Anoxic Event 2. *Geology* 49, 412–416.
- Clarkson M. O., Stirling C. H., Jenkyns H. C., Dickson A. J., Porcelli D., Moy C. M., von Strandmann P. A. E. P., Cooke I. R. and Lenton T. M. (2018) Uranium isotope evidence for two episodes of deoxygenation during Oceanic Anoxic Event 2. *Proc. Natl. Acad. Sci.* 115, 2918–2923.
- Cranston R. E. (1983) Chromium in Cascadia Basin, Northeast Pacific-Ocean. Mar. Chem. 13, 109–125.
- Connelly D. P., Statham P. J. and Knap A. H. (2006) Seasonal changes in speciation of dissolved chromium in the surface Sargasso Sea. *Deep Sea Res. Part I* 53, 1975–1988.
- Correa F. G., Becerril J. J. and Alcantara E. G. (2013) Study of Co (II) and Cr(VI) adsorption from aqueous solution by CaCO₃. *J. Chem. Soc. Pak.* **35**, 1088–1095.
- Cranston R. E. and Murray J. W. (1978) The determination of chromium species in natural waters. *Anal. Chim. Acta* 99, 275– 282
- Crowe S. A., Døssing L. N., Beukes N. J., Bau M., Kruger S. J., Frei R. and Canfield D. E. (2013) Atmospheric oxygenation three billion years ago. *Nature* 501, 535–538.
- Døssing L. N., Dideriksen K., Stipp S. L. S. and Frei R. (2011) Reduction of hexavalent chromium by ferrous iron: a process of chromium isotope fractionation and its relevance to natural environments. *Chem. Geol.* 285, 157–166.
- Du Vivier A. D., Selby D., Sageman B., Jarvia I., Grocke D. and Voigt S. (2014) Marine ¹⁸⁷Os/¹⁸⁸Os isotope stratigraphy reveals the interaction of volcanism and ocean circulation during Oceanic Anoxic Event 2. *Earth Planet. Sci. Lett.* **389**, 23–33.
- Eary L. E. and Rai D. (1987) Kinetics of chromium (III) oxidation to chromium (VI) by reaction with manganese dioxide. *Environ. Sci. Technol.* 21, 1187–1193.
- Elderfield H. (1970) Chromium speciation in seawater. *Earth Planet. Sci. Lett.* **9**, 10–16.
- Eldrett J. S., Minisini D. and Bergman S. C. (2014) Decoupling of the carbon cycle during Oceanic Anoxic Event 2. *Geology* 42, 567–570.
- Eldrett J. S., Ma C., Bergman S. C., Lutz B., Gregory F. J., Dodsworth P. and Kelly A. (2015a) An astronomically calibrated stratigraphic of the Cenomanian, Turonian and earliest Coniacian from the Cretaceous Western Interior Seaway, USA: Implications for global chronostratigraphy. *Cret. Res.* **56**, 316–344.
- Eldrett J. S., Ma C., Bergman S. C., Ozkan A., Minisini D., Lutz B. and Kelly S. J. (2015b) Origin of limestone-marlstone cycles: Astronomic forcing of organic rich sedimentary rocks from the Cenomanian to early Coniacian of the Cretaceous Western Interior Seaway, USA. Earth Planet. Sci. Lett. 423, 98–113.
- Eldrett J. S., Dodsworth P., Bergman S. C., Wright M. and Minisini D. (2017) Watermass evolution in the Cretaceous Western Interior Seaway of North America and Equatorial Atlantic. *Clim. Past* 13, 855–878.

- Ellis A. S., Johnson T. M. and Bullen T. D. (2002) Chromium isotopes and the fate of hexavalent chromium in the environment. *Science* **295**, 2060.
- Emerson S., Cranston R. E. and Liss P. S. (1979) Redox species in a reducing fjord: equilibrium and kinetic considerations. *Deep-Sea Res.* **26**, 859–878.
- Farkaš J., Fryda J., Paulukat C., Hathorne E. C., MatouśkováL Š., Rohovec J., Frydová B., Francová M. and Frei R. (2018) Chromium isotope fractionation between modern seawater and biogenic carbonates from the Great Barrier Reef, Australia: implications for the paleo-seawater δ⁵³Cr reconstruction. *Earth Planet. Sci. Lett.* 498, 140–151.
- Frei R., Gaucher C., Poulton S. W. and Canfield D. E. (2009) Fluctuations in Precambrian atmospheric oxygenation recorded by chromium isotopes. *Nature* **461**, 250–254.
- Füger A., Bruggmann S., Frei R., Leis A., Dietzel M. and Mavromatis V. (2019) The role of pH on Cr(VI) partitioning and isotopic fractionation during its incorporation in calcite. *Geochim. Cosmochim. Acta* 265, 520–532.
- Goring-Harford H. J., Klar J. K., Pearce C. R., Connelly D. P., Achterberg E. P. and James R. H. (2018) Behaviour of chromium isotopes in the eastern sub-tropical Atlantic Oxygen Minimum Zone. *Geochim. Cosmochim. Acta* 236, 41–59.
- Gilleaudeau G. J., Frei R., Kaufman A. J., Kah L. C., Azmy K., Bartley J. K., Chernyavskiy P. and Knoll A. H. (2016) Oxygenation of the mid-Proterozoic atmosphere: clues from chromium isotopes in carbonates. *Geochem. Perspect. Lett.*, 178–187.
- Gueguen B., Reinhard C. T., Algeo T. J., Peterson L. C., Nielsen S. G., Wang X., Rowe H. and Planavsky N. J. (2016) The chromium isotope composition of reducing and oxic marine sediments. *Geochim. Cosmochim. Acta* 184, 1–19.
- Halbach P., Holzbecher E., Koschinsky A., Michaelis W. and Seifert R. (2001) Deepsea hydrothermal microplume generation
 a case study from the North Fiji Basin. *Geomarine Lett.* 21, 94–102.
- Hawco N. J., Yang S.-C., Foreman R. K., Funkey C. P., Dugenne M., White A. E., Wilson S. T., Kelly R. L., Bian X., Huang K.-F., Karl D. M. and John S. G. (2020) Metal isotope signatures from lava-seawater interaction during the 2018 eruption of Kīlauea. *Geochim. Cosmochim. Acta* 282, 340–356.
- Huang T., Moos S. B. and Boyle E. A. (2021) Trivalent chromium isotopes in the eastern tropical North Pacific oxygen-deficient zone. *Proc. Natl. Acad. Sci.* 118 e1918605118.
- Holmden C., Jacobson A. D., Sageman B. B. and Hurtgen M.
 (2016) Response of the Cr isotope proxy to Cretaceous Ocean
 Anoxic Event 2 in a pelagic carbonate succession from the
 Western Interior Seaway. Geochim. Cosmochim. Acta 186, 277–
- Hover V. C., Walter L. M. and Peacor D. R. (2001) Early marine diagenesis of biogenic aragonite and Mg-calcite: new constrains from high-resolution STEM and AEM analysis of modern platform carbonate. *Chem. Geol.* 175, 221–248.
- Janssen D. J., Rickli J., Quay P. D., White A. E., Nasemann P. and Jaccard S. L. (2020) Biological control of chromium redox and stable isotope composition in the surface ocean. *Glob. Bio-geochem. Cycles* 34, e2019GB006397.
- Janssen D. J., Rickli J., Abbott A. N., Ellwood M. J., Twining B. S., Ohnemus D. C., Nasemann P., Gilliard D. and Jaccard S. L. (2021) Release from biogenic particles, benthic fluxes, and deep water circulation control Cr and d⁵³Cr distributions in the ocean interior. *Earth Planet. Sci. Lett.* 574 117163.
- Jeandel C. and Minster J. F. (1984) Isotope-dilution measurement of inorganic chromium (III) and total chromium in seawater. *Mar. Chem.* 14, 347–364.

- Jeandel C. and Minster J. F. (1987) Chromium behavior in the oceans: Global versus regional processes. *Global Biogeochem.* Cycles 1, 131–154.
- Jenkyns H. C., Dickson A. J., Ruhl M. and van den Boorn S. H. J. M. (2017) Basalt– seawater interaction, the Plenus Cold Event, enhanced weathering and geochemical change: deconstructing Oceanic Anoxic Event 2 (Cenomanian–Turonian, Late Cretaceous). Sedimentology 64, 16–43.
- Jones M. M., Sageman B. B., Selby D., Jicha B. R., Singer B. S. and Titus A. L. (2020) Regional chronostratigraphic synthesis of the Cenomanian-Turonian OAE 2 interval Western Interior Basin (USA): New Re-Os chemostratigraphy and ⁴⁰Ar/³⁹Ar geochronology. GSA Bull. 133, 1090–1104.
- Johnson A. and Cronan D. S. (2001) Hydrothermal metalliferous sediments and waters off the Lesser Antilles. *Mar. Georesources* and Geotech. 19, 65–83.
- Klaebe R., Swart P. and Frei R. (2021) Chromium isotope heterogeneity on a modern carbonate platform. Chem. Geol., 120227.
- Marques Fernandes M., Schmidt M., Stumpf T., Walther C., Bosbach D., Klenze R. and Fanghänel T. (2008) Site-selective time-resolved laserfluorescence spectroscopy of Eu³⁺ in calcite. *J. Colloid Interface Sci.* **321**, 323–331.
- Miletto M., Wang X. L., Planavsky N. J., Luther G. W., Lyons T. W. and Tebo B. M. (2021) Marine microbial Mn(II) oxidation mediates Cr(III) oxidation and isotope fractionation. *Geochim. Cosmochim. Acta* **297**, 101–119.
- Minisini D., Eldrett J., Bergman S. C. and Forkner R. (2018) Chronostratigraphic framework and depositional environments in the organic-rich, mudstone-dominated Eagle Ford Group, Texas, USA. *Sedimentology* **65**, 1520–1557.
- Moos S. B. and Boyle E. A. (2019) Determination of accurate and precise chromium isotope ratios in seawater samples by MC-ICP-MS illustrated by analysis of SAFe Station in the North Pacific Ocean. *Chem. Geol.* 511, 481–493.
- Mugo R. K. and Orians K. J. (1993) Seagoing method for the determination of chromium(III) and total chromium in sea water by electron-capture detection gas chromatography. *Anal. Chim. Acta* 271, 1–9.
- Murray J. W., Spell B. and Paul B. (1983) The contrasting geochemistry of manganese and chromium in the eastern tropical Pacific Ocean. In *Trace Metals in Sea Water*. Springer, pp. 643–669.
- Nakayama T., Tsurubo S., Tokoro H. and Fujinaga T. (1981) Chemical speciation of chromium in sea water Part 1. Effect of naturally occurring organic materials on the complex formation of chromium (III). *Anal. Chim. Acta* **130**, 289–294.
- Nana Yobo L., Brandon A. D., Holmden C., Lau K. V. and Eldrett J. (2021) Changing inputs of continental and submarine weathering sources of Sr to the oceans during OAE 2. Geochim. Cosmochim. Acta 303, 205–225.
- Nasemann P., Janssen D. J., Rickli J., Grasse P., Franck M. and Jaccard S. L. (2020) Chromium reduction and associated stable isotope fractionation restricted to anoxic shelf waters in the Peruvian Oxygen Minimum Zone. *Geochim. Cosmochim. Acta* 285, 207–224.
- O'Connor L. K., Jenkyns H. C., Robinson S. A., Remmelzwaal S. R., Batenburg S. J., Parkinson I. J. and Gale A. S. (2020) A reevaluation of the Plenus Cold Event, and the links between CO₂, temperature, and seawater chemistry during OAE 2. *Paleoceanogr. Paleoclimatol.* **35**(4), e2019PA003631.
- Orth C. J., Attrep, Jr., M., Quintana L. R., Elder W. P., Kauffman E. G., Diner R. and Villamil T. (1993) Elemental abundance anomalies in the late Cenomanian extinction interval: a search for the source(s). *Earth Planet. Sci. Lett.* 117, 189–204.

- Outka D. E. and Williams D. C. (1971) Sequential coccolith morphogenesis in *Hymenomonas carterae*. J. Protozool. 18, 285–297.
- Paez-Reyes M., Carvajal-Ortiz H., Sahoo S. K., Varol O., Miller V.
 B., Hughes G. W., Gaona-Narvaez T., Patarroyo G. D., Curtis J. H., Lerma I. and Copeland P. (2021) Assessing the contribution of the La Luna Sea to the global sink of organic carbon during the Cenomanian-Turonian Oceanic Anoxic Event 2 (OAE2). Glob. Planet. Change 199 103424.
- Peucker-Ehrenbrink B. and Fiske G. J. (2019) A continental perspective of the seawater ⁸⁷Sr/⁸⁶Sr record: a review. *Chem. Geol.* **510.** 140–165.
- Planavsky N. J., Reinhard C. T., Wang X., Thomson D., McGoldrick P., Rainbird R. H., Johnson T., Fischer W. W. and Lyons T. W. (2014) Low Mid-Proterozoic atmospheric oxygen levels and the delayed rise of animals. *Science* 346, 635– 638
- Pereira N. S., Voegelin A. R., Paulukat C., Sial A. N., Ferreira V. P. and Frei R. (2016) Chromium-isotope signatures in scleractinian corals from the Rocas Atoll, tropical South Atlantic. *Geobiology* 14, 54–67.
- Pettine M. and Millero F. J. (1990) Chromium speciation in seawater: the probable role of hydrogen peroxide. *Limnol. Oceanogr.* **35**, 730–736.
- Polyak B. G., Bouysse P. h., Kononov V. I., Butuzova G. N., Criaud A., Dvorov V. I., Khutorskoy M. D., Matveev V. G., Paduchikh V. I., Radionova E. P., Rot A. A., Tolstikhin I. N., Voznesensky A. I. and Zverev V. P. (1992) Evidence of submarine hydrothermal discharge to the north west of Guadeloupe Island (Lesser Antilles island arc). J. Volcanol. Geotherm. Res. 54, 81–105.
- Remmelzwaal S. R. C., Sadekov A. Y., Parkinson I. J., Schmidt D. N., Titelboim D. and Abramovich S. (2019) Post-depositional overprinting of chromium in foraminifera. *Earth Planet. Sci. Lett.* **515**, 100–111.
- Reinhard C., Planavsky N., Wang X., Fischer W., Johnson T. and Lyons T. W. (2014) The isotopic composition of authigenic chromium in anoxic marine sediments: a case study from the Cariaco basin. *Earth Planet. Sci. Lett.* 407, 9–18.
- Rickli J., Janssen D. J., Hassler C., Ellwood M. J. and Jaccard S. L. (2019) Chromium biogeochemistry and stable isotope distribution in the Southern Ocean. *Geochim. Cosmochim. Acta* 262, 188–206.
- Rue E. L., Smith G. J., Cutter G. A. and Bruland K. W. (1997) The response of trace element redox couples to suboxic conditions in the water column. *Deep-Sea Res. Part* 144, 113–134.
- Saad E. M., Wang X., Planavsky N. J., Reinhard C. T. and Tang Y. (2017) Redox-independent chromium isotope fractionation induced by ligand-promoted dis-solution. *Nat. Commun.* 8, 1– 10
- Sageman B. B., Meyers S. R. and Arthur M. A. (2006) Orbital time scale and new C-isotope record for Cenomanian-Turonian boundary stratotype. *Geology* 34, 125–128.
- Sander S. G. and Koschinsky A. (2000) Onboard-ship redox speciation of chromium in diffuse hydrothermal fluids from the North Fiji Basin. *Mar. Chem.* 71, 83–102.
- Sander S., Koschinsky A. and Halbach P. (2003) Redox speciation of chromium in the oceanic water column of the Lesser Antilles and offshore Otago Peninsula, New Zealand. *Mar. Freshwater Res.* 54, 745–775.
- Scheiderich K., Amini M., Holmden C. and Francois R. (2015) Global variability of chromium isotopes in seawater demonstrated by Pacific, Atlantic and Arctic Ocean samples. *Earth Planet. Sci. Lett.* **423**, 87–97.

- Schlanger S. O. and Jenkyns H. C. (1976) Cretaceous oceanic anoxic events. Causes and consequences: Geol. Mijnbouw 55, 179–184.
- Schoenberg R., Zink S., Staubwasser M. and von Blanckenburg F. (2008) The stable Cr isotope inventory of solid Earth reservoirs determined by double spike MC-ICP-MS. *Chem. Geol.* 249, 294–306.
- Schröder-Adams C. J., Herrle J. O., Selby D., Quesnel A. and Froude G. (2019) Influence of the High Arctic Igneous Province on the Cenomanian/Turonian boundary interval, Sverdrup Basin, High Canadian Arctic. *Earth Planet. Sci. Lett.* 511, 76– 88
- Schroeder D. S. and Lee G. F. (1975) Potential transformations of chromium in natural waters. *Water Air Soil Pollut.* **4**, 355–365.
- Scotese C. (2016) PALEOMAP PaleoAtlas for GPlates and the PaleoData Plotter Program, PALEOMAP Project. http://www.earthbyte.org/paleomap-paleoatlas-for-gplates/.
- Semeniuk D. M., Maldonado M. T. and Jaccard S. L. (2016) Chromium uptake and adsorption in marine phytoplankton – Implications for the marine chromium cycle. *Geochim. Cosmochim. Acta* 184, 41–54.
- Sirinawin W., Turner D. R. and Westerlund S. (2000) Chromium (VI) distributions in the Arctic and the Atlantic Oceans and a Reassessment of the oceanic Cr cycle. Mar. Chem. 71, 265–282.
- Sharma M., Rosenberg E. J. and Butterfield D. A. (2007) Search for the proverbial mantle osmium sources to the oceans: hydrothermal alteration of mid-ocean ridge basalt. *Geochim. Cosmochim. Acta* 71, 4655–4667.
- Sikora E. R., Johnson T. M. and Bullen T. D. (2008) Microbial mass-dependent fractionation of chromium isotopes. *Geochim. Cosmochim. Acta* 72, 3631–3641.
- Sinton C. W. and Duncan R. A. (1997) Potential links between ocean plateau volcanism and global ocean anoxia at the Cenomanian-Turonian boundary. *Econ. Geol.* **92**, 836–842.
- Snow L. J., Duncan R. A. and Bralower T. J. (2005) Trace element abundances in the Rock Canyon Anticline, Pueblo, Colorado, marine sedimentary section and their relationship to Caribbean plateau construction and oxygen anoxic event 2. *Paleoceanogr. Paleoclimatol.* 20, PA3005.
- Sullivan D. L., Brandon A. D., Eldrett J., Bergman S. C., Wright S. and Minisini D. (2020) High resolution osmium data record three distinct pulses of magmatic activity during cretaceous

- Oceanic Anoxic Event 2 (OAE 2). Geochim. Cosmochim. Acta 285 257273.
- Sweere T. C., Dickson A. J., Jenkyns H. C., Porcelli D. and Henderson G. M. (2020) Zinc and cadmium-isotope evidence for redox-driven perturbations to global micronutrient cycles during Oceanic Anoxic Event 2 (Late Cretaceous). *Earth Planet. Sci. Lett.* 546, 251–262.
- Toma J., Holmden C., Shakotko P., Pan Y. and Ootes L. (2019) Cr isotopic insights into ca. 1.9Ga oxidative weathering of the continents using the Beaverlodge Lake paleosol, Northwest Territories, Canada. *Geobiology* 17, 467–489.
- Trabucho Alexandre J., Tuenter E., Henstra G. A., van der Zwan K. J., van de Wal R. S. W., Dijkstra H. A. and de Boer P. L. (2010) The mid-Cretaceous North Atlantic nutrient trap: Black shales and OAEs. *Paleoceanography* 25, PA4201.
- Turgeon S. C. and Creaser R. A. (2008) Cretaceous Anoxic Event 2 triggered by a massive magmatic episode. *Nature* 454, 323–326.
- van Helmond N. A. G. M., Sluijs A., Reichart G.-J., Damste Å. L., Sinninghe J. S., Slomp C. P. and Brinkhuis H. (2014) A perturbed hydrological cycle during Oceanic Anoxic Event 2. *Geology* **42**, 123–126.
- Wang X., Reinhard C. T., Planavsky N. J., Owens J. D., Lyons T. W. and Johnson T. M. (2016) Sedimentary chromium isotopic compositions across the Cretaceous OAE 2 at Demerara Rise Site 1258. Chem. Geol. 429, 85–92.
- Wang C., Reinhard C. T., Rybacki K. S., Hardisty D. S., Ossa Ossa F., Wang X., Hofmann A., Asael D., Robbins L. J., Zhang L. and Planavsky N. J. (2021) Chromium isotope systematics and the diagenesis of marine carbonates. *Earth Planet. Sci. Lett.* 562 116824.
- Zink S., Schoenberg R. and Staubwasser M. (2010) Isotopic fractionation and reaction kinetics between Cr (III) and Cr (VI) in aqueous media. *Geochim. Cosmochim. Acta* **74**, 5729–5745.
- Zheng X.-Y., Jenkyns H. C., Gale A. S., Ward D. J. and Henderson G. M. (2013) Changing Ocean circulation and hydrothermal inputs during Oceanic Anoxic Event 2 (Cenomanian–Turonian): evidence from Nd-isotopes in the European shelf sea. *Earth Plan. Sci. Lett.* 375, 338–348.

Associate editor: Aubrey Zerkle